PLOS ONE

RESEARCH ARTICLE

The evolving systemic biomarker milieu in obese ZSF1 rat model of human cardiometabolic syndrome: Characterization of the model and cardioprotective effect of GDF15

Marina Stolina[1], Xin Luo[2], Denise Dwyer[1], Chun-Ya Han[1], Rhonda Chen[3], Ying Zhang[3], YuMei Xiong[3], Yinhong Chen[3], Jun Yin[2], Artem Shkumatov[4], Brandon Ason[3], Clarence Hale[1], Murielle M. Véniant[1]*

1 Amgen Research, Department of Cardiometabolic, Thousand Oaks, California, United States of America, **2** Amgen Research, Genome Analysis Unit, San Francisco, California, United States of America, **3** Amgen Research, Department of Cardiometabolic, San Francisco, California, United States of America, **4** Amgen Research, Department of Translational and Bioanalytical Sciences, San Francisco, California, United States of America

* mveniant@amgen.com

Abstract

Cardiometabolic syndrome has become a global health issue. Heart failure is a common comorbidity of cardiometabolic syndrome. Successful drug development to prevent cardiometabolic syndrome and associated comorbidities requires preclinical models predictive of human conditions. To characterize the heart failure component of cardiometabolic syndrome, cardiometabolic, metabolic, and renal biomarkers were evaluated in lean and obese ZSF1 19- to 32-week-old male rats. Histopathological assessment of kidneys and hearts was performed. Cardiac function, exercise capacity, and left ventricular gene expression were also analyzed. Obese ZSF1 rats exhibited multiple features of human cardiometabolic syndrome by pathological changes in systemic renal, metabolic, and cardiovascular disease circulating biomarkers. Hemodynamic assessment, echocardiography, and decreased exercise capacity confirmed heart failure with preserved ejection fraction. RNA-seq results demonstrated changes in left ventricular gene expression associated with fatty acid and branched chain amino acid metabolism, cardiomyopathy, cardiac hypertrophy, and heart failure. Twelve weeks of growth differentiation factor 15 (GDF15) treatment significantly decreased body weight, food intake, blood glucose, and triglycerides and improved exercise capacity in obese ZSF1 males. Systemic cardiovascular injury markers were significantly lower in GDF15-treated obese ZSF1 rats. Obese ZSF1 male rats represent a preclinical model for human cardiometabolic syndrome with established heart failure with preserved ejection fraction. GDF15 treatment mediated dietary response and demonstrated a cardioprotective effect in obese ZSF1 rats.

OPEN ACCESS

Citation: Stolina M, Luo X, Dwyer D, Han C-Y, Chen R, Zhang Y, et al. (2020) The evolving systemic biomarker milieu in obese ZSF1 rat model of human cardiometabolic syndrome: Characterization of the model and cardioprotective effect of GDF15. PLoS ONE 15(8): e0231234. https://doi.org/10.1371/journal.pone.0231234

Editor: Jaap A. Joles, University Medical Center Utrecht, NETHERLANDS

Received: March 17, 2020

Accepted: August 3, 2020

Published: August 17, 2020

Data Availability Statement: All relevant data are within the manuscript and its Supporting Information files.

Funding: This study was funded by Amgen Inc. Beyond the named authors, who are employees of Amgen, the sponsor reviewed the manuscript but had no role in study design, data collection and analysis, decision to publish, or preparation of the manuscript and only provided financial support in the form of authors' salaries [MS, XL, DD, C-YH,

RC, YZ, YMX, YC, JY, AS, BA, CH, MMV] and research materials. The specific roles of these authors are articulated in the 'Author Contributions' section.

Competing interests: All authors are employees and stockholders of Amgen Inc., with no other competing interests to disclose. This relationship does not alter our adherence to PLOS ONE policies on sharing data and materials.

Introduction

Cardiometabolic syndrome (CMS)—a condition that encompasses impaired metabolism (insulin resistance [IR], impaired glucose tolerance), dyslipidemia, hypertension, renal dysfunction, central obesity, and heart failure (HF)—is now recognized as a disease by the World Health Organization (WHO) and the American Society of Endocrinology [1]. Obesity and diabetes mellitus comorbidities are associated with progressive left ventricular (LV) remodeling and dysfunction. Also, these comorbidities are commonly observed in HF with preserved ejection fraction (HFpEF) [2]. Results from a recent epidemiological study (cohort of 3.5 million individuals) demonstrated an incremental increase in the hazard ratio (HR) for HF; HRs were 1.8 in normal weight individuals with three metabolic abnormalities, 2.1 in overweight individuals with three metabolic abnormalities, and up to 3.9 in obese individuals with three metabolic abnormalities. Incidence of HFpEF, which currently represents approximately 50% of all HF cases, continues to rise and its prognosis fails to improve partly due to the lack of therapies available to treat this disease [3].

An important step in the development of novel therapeutic agents against CMS is the establishment of a preclinical model that represents a cluster of cardiometabolic disturbances that are similar to those of the human condition. The obese ZSF1 rat model (generated by crossing lean, non-hypertensive, female Zucker diabetic fatty rats [ZDF, +/*fa*] with lean, spontaneously hypertensive, HF-prone male rats [SHHF/Mcc, +/*facp*]) [4] exhibits features and complications that resemble what is observed in human CMS [5, 6]. Twenty-week-old obese ZSF1 male rats developed diastolic dysfunction based on prolonged τ and elevated end-diastolic pressure-volume relationship (EDPVR), and showed exercise intolerance, which is an important feature of human HFpEF [7]. Although both lean and obese ZSF1 rats, by inheritance of a hypertensive gene, showed elevated blood pressure [4], only 20-week-old obese ZSF1 males demonstrated LV hypertrophy, left atrial (LA) dilation, and increased myocardial stiffness due to myofilament changes [8]. In a recent study it was shown that, at 26 weeks of age, both ZSF1 males and females exhibited comparable impaired cardiac function and diastolic dysfunction [9].

Growth differentiation factor 15 (GDF15), also called macrophage inhibitory cytokine (MIC-1), is a distant member of the transforming growth factor β (TGF-β) superfamily. GDF15 is a homodimeric secreted protein with a mass of 25 kDa [10, 11]. Circulating levels are increased in humans with metabolic syndrome [12] and in those with increased risk of cardiovascular disease (CVD) [13, 14]. Recently published studies in obese preclinical models demonstrated an aversive dietary response to GDF15 treatment, leading to an improvement in metabolic parameters. Thus, daily injections of GDF15 to mice for 14 days to 21 weeks resulted in significantly reduced body weight and food intake, increased energy expenditure, improved glucose tolerance, and reduced inflammatory cytokines [15]. Administration of human GDF15 to rodents via an adenovirus system and to obese monkeys via protein injections led to body weight loss and an improved metabolic profile [16]. Treatment of obese mice with a human GDF15-Fc fusion protein (Fc-GDF15) led to reduced appetite and body weight and a shift of metabolic parameters toward lipid oxidation [16–19]. Weekly administration of Fc-GDF15 to obese cynomolgus monkeys for 28–42 days resulted in significantly reduced body weight and food consumption, lower serum triglyceride levels, and improved serum insulin [16, 20]. To date, GDF15 is shown to have mediated aversive dietary response, influenced the governance of systemic energy balance, and prevented obesity through enhanced thermogenesis and oxidative metabolism [21, 22].

While impaired metabolism, LV hypertrophy, LA dilation, increased myocardial stiffness, decreased exercise capacity, and histological analysis of cardiac hypertrophy and fibrosis of

obese ZSF1 male rats have been published in several separate scientific reports [5, 8, 23], the obesity-induced changes in systemic cardiovascular protein biomarkers and LV gene expression have not been documented, analyzed, and reported to date. In the current study, we performed a comprehensive comparative evaluation of 20- to 22-week-old male lean and obese ZSF1 rats by systematically studying the metabolic, renal, and cardiovascular protein biomarkers. We also used echocardiography, invasive hemodynamic and exercise capacity assessments, and LV gene expression analysis to complete the characterization of this animal model. After establishing and extensively characterizing the ZSF1 rats, we investigated whether 12 weeks of treatment with Fc-GDF15 in 22-week-old obese ZSF1 males would result in decreased body weight and food intake and improvement in metabolic profile, similar to prior non-clinical studies [16, 19], and also whether a cardioprotective effect could be demonstrated by improving exercise capacity and circulating levels of cardiovascular protein biomarkers.

Materials and methods

Animal welfare and husbandry

All studies were performed in accordance with the Institutional Animal Care and Use Committee guidelines and complied with the Final Rules of the Animal Welfare Act regulations (Code of Federal Regulations, Title 9), the Public Health Service Policy on Humane Care and Use of Laboratory Animals in the Office of Laboratory Animal Welfare (2002), and the Guide for the Care and Use of Laboratory Animals from the National Research Council (1996). All rodent studies were conducted at Amgen Inc and were approved by the Amgen Institutional Animal Care and Use Committee (IACUC). Animals were maintained in rooms with a 12-hour light/dark cycle, temperature of 22˚C, and humidity of 30–70%. Animals had free access to food and water and were maintained on standard rodent chow unless otherwise indicated. Rats were single-housed at Amgen's Association for Assessment and Accreditation of Laboratory Animal Care (AAALAC)–accredited facility in filter-top cages on corn cob bedding, with ad libitum access to pelleted feed (Harlan/Teklad Irradiated Global Soy Protein-Free Extruded Rodent Diet 2920x; Harlan, Madison, WI, USA) and reverse-osmosis purified water via an automatic watering system. Animals were maintained in pathogen-free conditions with a 12-hour light/dark cycle and had access to enrichment opportunities.

In vivo study design for characterization of obese ZSF1 rat as a preclinical model of human CMS

Eighteen-week-old lean ZSF1 (strain 379) and obese ZSF1 (strain 378) rats were purchased from Charles River Laboratories (Kingston, NY, USA) and single-housed at Amgen's AAALAC-accredited facility. After 2 weeks of acclimation, both groups of rats (n = 8 per group for males; n = 12 per group for females) were subjected to blood collection via tail vein, echocardiography, hemodynamic assessment, and evaluation of exercise endurance (time and distance) using a treadmill. A separate cohort from the same batch of acclimated obese ZSF1 (n = 6) and lean ZSF1 (n = 6) rats was subjected to heart isolation, RNA extraction, and gene expression analysis.

In vivo study design for the evaluation of Fc-GDF15 treatment effect on CMS-specific biomarkers in obese ZSF1 rats

Twenty-week-old obese ZSF1 male rats (strain 378, n = 30) were purchased from Charles River Laboratories, single-housed at Amgen's AAALAC-accredited facility, and acclimated for 2 weeks. At 22 weeks of age, baseline blood collection (for metabolic biomarker evaluation)

and body weight assessment were performed for every animal. Twenty-four hours later, the rats were randomized into two groups and injected subcutaneously once a week for 12 weeks with either A5.2Su buffer (vehicle group, $n = 15$) or 1.5 mg/kg DhCpmFc-(G4S)4-hGDF15 [16] (Fc-GDF15 group, $n = 15$). DhCpmFc-(G4S)4-hGDF15 is a fusion protein with one GDF15 subunit per Fc dimer that have complementary charges in the CH3 domains of the Fc region. We will refer to this molecule as Fc-GDF15. For the duration of the study, every rat was subjected to weekly blood collection, food intake, and body weight assessments. At the end of the study, rats from both treatment groups were subjected to echocardiography, hemodynamic assessment, and evaluation of exercise endurance (time and distance) using treadmill equipment. The biological half-life of Fc-GDF15 is ~3 days, and our pharmacokinetic analysis indicated that Fc-GDF15 at 1.5 mg/kg is suitable for weekly dosing [16]. The dose of 1.5 mg/kg of Fc-GDF15 led to the development of anti-drug antibody in three out of 15 obese ZSF1 rats. These three animals were excluded from the study analysis, and the final number of obese ZSF1 males in the FcGDF15–treated group was 12.

Histopathology of kidneys and hearts from lean and obese ZSF1 rats

Kidneys from 19- to 21-week-old lean ($n = 3$) and obese ($n = 6$) male ZSF1 rats were fixed overnight in 10% neutral buffered formalin and were processed and embedded in paraffin. The 4 μm sections were prepared and stained with standard hematoxylin and eosin. Hearts from 20-week-old obese ($n = 9$) and 32-week-old lean (n = 4) and obese ($n = 5$) male ZSF1 rats were fixed overnight in 10% neutral buffered formalin and were processed and embedded in paraffin. The 4 μm sections were prepared and stained with standard hematoxylin and eosin or Picrosirius red (for collagen staining). Standard histopathological evaluation of above tissues was performed by a board-certified veterinary pathologist using Olympus BX60 light microscope. For quantitative evaluation of cardiac collagen, the slides stained with Masson's trichrome were scanned at 40X using high-volume digital whole slide scanning system Leica AT2 (Leica Biosystems, Wetzlar, Germany), and the percentage of positively stained tissue area was determined using Visiopharm image analysis software (2019.02.2.6239 version; Visiopharm, Hørsholm, Denmark).

Cardiovascular, kidney injury, and metabolic biomarkers in serum/plasma

Animals were fasted for 4 hours prior to blood collection. The first 0.5 mL aliquot of whole blood was collected from the tail vein into serum separator tubes (Microtainer, Becton Dickinson, Franklin Lakes, NJ, USA), and the second 0.5 mL aliquot of whole blood into ethylenediaminetetraacetic acid (EDTA) plasma separation tubes (Microtainer, Becton Dickinson, Franklin Lakes, NJ). Separated serum/plasma was aliquoted and stored at –80˚C. Blood glucose levels were measured using AlphaTrak 2 glucose strip (Abbott Laboratories, Lake Bluff, IL, USA). Blood insulin was evaluated using a rat insulin enzyme-linked immunosorbent assay (ELISA) kit (Alpco, Salem, NH, USA). Serum triglyceride and cholesterol levels were measured weekly by triglyceride quantitation kits (Fisher Diagnostics, Middletown, VA, USA). Systemic levels of GDF15 were evaluated with a commercial ELISA kit (R&D Systems, Minneapolis, MN, USA) specific for rat GDF15 with no detected cross-reactivity with human GDF15 or GDF11 (according to the manufacturer data sheet). Circulating proinsulin levels in serum/plasma of 20-week-old ZSF1 male rats were evaluated with a commercial ELISA kit (Mercodia, Uppsala, Sweden). A limited array of circulating metabolic hormones (amylin [active], C-peptide 2, ghrelin [active], gastric inhibitory polypeptide [GIP, total], glucagon-like peptide 1 [GLP-1, active], glucagon, interleukin-6 [IL-6], leptin, pancreatic polypeptide [PP], and peptide YY [PYY]) was assessed in serum/plasma collected from lean and obese ZSF1 rats at the

age of 20 weeks by rat-specific MILLIplex kit (Millipore, Billerica, MA, USA). Kidney injury markers KIM-1 and NGAL were evaluated in serum from 20-week-old lean and obese ZSF1 rats by multiplex MILLIplex kits (Millipore). Serum NT-proBNP and rat cardiac injury markers (fatty-acid-binding protein 3 [FABP3] and myosin light chain 3 [Myl3]) were measured by using rat-specific single-plex or multiplex commercial assays from Meso Scale Diagnostics (Rockville, MD, USA). Systemic levels of vascular markers were evaluated at the end of the Fc-GDF15 and vehicle treatment of obese ZSF1 rats by using multiplex MILLIplex kits (Millipore). The rat vascular injury panels included VEGF, MCP1, TIMP1, ST2 (IL1RL1), TNFα, vWF, adiponectin, sE-selectin, and sICAM1. Systemic aldosterone levels were measured by enzyme immunoassay (m/r/h Aldosterone ELISA; Enzo Life Sciences, Farmingdale, NY, USA) and serum osteopontin (OPN) by Rat Single Plex Kit (Millipore). All the assays were performed in accordance with manufacturer protocols.

RNA isolation and sequencing analysis of left heart

At scheduled necropsy, LA and LV of the heart were washed briefly in RNase-free saline, placed in cryo-tubes, snap-frozen in liquid nitrogen, and stored at –80˚C. Samples were subjected to dry pulverization before being homogenized in buffer (350 μL of Qiagen RLT buffer with 1% β-mercaptoethanol; Qiagen, Germantown, MD, USA). The homogenate was transferred to an RNase-free 1.5 mL centrifuge tube, after which 590 μL RNase-free water and 10 μL of a 20 mg/mL proteinase K solution were added. Samples were incubated at 55˚C for 10 minutes, centrifuged, and the supernatant collected. RNA was then extracted using RNeasy Micro Kit (Qiagen) with on-column DNase treatment (Qiagen) according to the manufacturer's instructions. RNA concentration and integrity were assessed using a Bioanalyzer (Agilent, Santa Clara, CA, USA). Samples with $\geq$80 ng total RNA and RNA integrity numbers (RIN) $\geq$7 were used for sequencing. Raw reads were processed using OmicSoft (Cary, NC, USA) Array Studio software (Oshell.exe v10.0) [24]. The expression level was expressed as fragments per kilobase per million quantile normalized (FPKQ) values, which were generated using OmicSoft's implementation of the RSEM algorithm and normalized using upper-quartile normalization [25].

Differential expression and pathway analysis

Differential expression analysis was performed using DESeq2 v1.10.1 for obese vs lean ZSF1 LV comparison [26], and gene expression fold changes were calculated using FPKQ values. Genes with Benjamini-Hochberg corrected p-value < 0.05 and fold change between the two conditions ≥ 1.5 or ≤ 0.67 were selected as significantly differentially expressed genes (DEGs).

The analysis of the genes that have human homologue and are abundant in human heart (top three out of 45 tissue roll-ups with median FPKQ ≥ 1) was based on Genotype-Tissue Expression (GTEX) data [27]. Heart abundant altered genes were visualized in a graphic heatmap using the ComplexHeatmap R package [28]. All the DEGs and heart abundant DEGs were further annotated by ingenuity pathway analysis (IPA; QIAGEN, Redwood City, CA, USA). Metabolic signaling pathway enrichment was done on the significantly DEGs by an adjusted p-value cutoff of 0.05 by IPA. Gene expression enrichment in diseases was analyzed by using Medical Subject Headings (MeSH) terms using the meshes R package [29]. Dotplots and heatplots were generated with clusterProfiler [30].

Echocardiography

Non-invasive echocardiograms were obtained on anesthetized rats (isoflurane, 3% induction, 1.5% maintenance) using a Vevo 2100 imaging system (FUJIFILM VisualSonics, Inc, Toronto,

Canada). Animals were shaved and placed on a platform, and a thermo-couple probe was used to assess body temperature and to adjust the temperature of the platform to maintain normothermia. Sonography gel was applied on the thorax. Two-dimensional targeted B-mode and M-mode imaging was obtained from the long-axis and short-axis views at the level of the papillary muscle. Coronary flow was measured by pulsed-wave (PW) Doppler, and movement of the LV wall was measured by tissue Doppler by placing the probe to the chest and focusing the image on the ventricular wall region to achieve an apical four-chamber view. Animals were subsequently wiped clean of sonography gel, allowed to achieve consciousness, and returned to their home cage.

Invasive hemodynamic assessment

Animals underwent general anesthesia using ketamine/diazepam (intraperitoneal) injection (80–100 mg/kg ketamine; 5–10 mg/kg diazepam) followed by a ketamine boost (10–20 mg/kg) as necessary to maintain the anesthesia plane. Anesthetized animals had the surgical sites shaved with a small animal shear. Animals were then placed on a heated surgical platform, and body temperature was monitored and maintained throughout the study via a rectal probe. Arterial pressure was measured via femoral artery catheterization (SPR-839; Millar, Houston, TX, USA). An incision in the medial aspect of the leg was made, and the fat overlaying the femoral vessels and femoral nerve in the area between the abdominal wall and the upper leg was gently teased apart using forceps or Q-tips. The fascia overlying the artery, nerve, and vein was removed. The artery was isolated and ligated by a distal suture, and a loose tie was held in place using a hemostat. A microvessel clip or suture was placed on the artery near the abdominal wall, and a small incision was made into the vessel using Vannas micro-scissors or a 25-gauge needle. The clip was released by one hand, and the Millar catheter was advanced quickly into the femoral artery, followed by the tightening of the proximal suture to prevent blood loss. Pressure was then recorded. LV pressure and volume were measured via carotid artery catheterization (SPR-838; Millar). The right carotid artery was isolated, and a suture was tied around the vessel approximately 0.25 cm below the skull base to disrupt blood flow. A suture was placed around the artery near the rib cage and held in place using a hemostat. A small incision was made into the vessel using Vannas micro-scissors or a 25-gauge needle. The clip was released by one hand, and the Millar catheter was advanced quickly into the carotid artery, followed by the tightening of the proximal suture to prevent blood loss. The catheter was advanced until it entered the LV for pressure-volume loop measurement. Animals were euthanized under anesthesia after completion of the data acquisition.

Treadmill assessment

Rats were subjected to evaluation of exercise endurance (time and distance) using a treadmill. Endurance exercise performance was estimated using two parameters: run duration (minutes) and distance (meters). Oxygen consumption, an indicator of exercise capacity, was measured by monitoring the O_2 concentration of expired air. Peak chamber oxygen decrement, which usually occurs just prior to exhaustion, was used to calculate and define the animal's peak volume of oxygen consumption (VO_2). The contribution of anaerobic metabolism to overall energy production during exercise was estimated by calculating the respiratory exchange ratio (RER), the ratio of VO_2 to VCO_2 (the amount of CO_2 within the chamber just prior to exhaustion). Rats were initially familiarized to the motorized rodent treadmill (Columbus Instruments, Columbus, OH, USA) for 5 days before completing the exercise performance test. Rats were placed on the treadmill and allowed to adapt to the surroundings for 2–5 minutes before starting. Familiarization runs consisted of 10 minutes of

running on an incline of 10˚ at a speed of 12 m/min. For the treadmill challenge, rats were placed on the treadmill and allowed to adapt to the surroundings for 2–5 minutes before starting. The treadmill was initiated at a speed of 8.5 m/min with a 0˚ incline. After 3 minutes, the speed and incline were raised up to 10 m/min. The speed was subsequently increased progressively by 2.5 m/min every 3 minutes. The incline was progressively increased by 5˚ every 9 minutes to a maximum of up to 30˚. Exercise continued until exhaustion, which is defined as the inability to maintain running speed despite repeated contact with the electric grid (three shocks in less than 15 seconds).

Statistical analysis

Results for serum protein biomarkers, hemodynamic assessments, echocardiography, and systemic metabolic parameters are expressed as mean ± standard error of the mean (SEM). Differences between the two groups were examined between lean ZSF1 and obese ZSF1 rats of the same age or at the end of the Fc-GDF15 treatment (week 12) between vehicle-treated and Fc-GDF15–treated obese ZSF1 rats. Unpaired Student's *t* test was performed to evaluate the statistical significance between the groups. When the effect in vehicle-treated and Fc-GDF15–treated obese ZSF1 rats was studied longitudinally (0–12 weeks), a two-way ANOVA with Sidak's multiple comparison test was performed for metabolic parameters, body weight, and food intake. A value of $p < 0.05$ was used to determine statistical significance. Stars (*) indicate significance: * $p < 0.05$, ** $p < 0.01$, *** $p < 0.001$, **** $p < 0.0001$. All statistical analyses were performed by using GraphPad Prism (version 8.4.3, GraphPad Software, San Diego, CA, USA).

Results

At the age of 20 weeks, obese ZSF1 male rats exhibited increased body weight and impaired metabolism

We have confirmed previous reports [4] and demonstrated that 20-week-old obese ZSF1 rats exhibit impaired markers of metabolism (Fig 1A–1G, S1 Table), including elevated body weight (38% increase vs lean group; $p < 0.0001$) and significantly increased blood glucose (1.6-fold; $p = 0.0060$), serum insulin (14.7-fold; $p = 0.0019$), cholesterol (2.9-fold; $p < 0.0001$), and triglyceride (15-fold; $p < 0.0001$) levels relative to lean ZSF1 littermate controls. Significant decrease in serum adiponectin from 2.6 ± 0.09 μg/mL in lean ZSF1 serum to 1.9 ± 0.05 μg/mL in obese ZSF1 serum ($p < 0.0001$) indicated deposition of newly formed fat and served as a reliable obesity biomarker. In concert with human data, GDF15 levels were significantly increased in the serum of obese ZSF1 rats (Fig 1G).

Twenty-week-old obese ZSF1 male rats demonstrated pancreatic and renal dysfunction

Since the array of biomarker changes relevant to the progression and establishment of CMS in humans includes type 2 diabetes (T2D) and renal impairment, we evaluated systemic levels of major pancreatic and kidney injury biomarkers in obese ZSF1 rats compared with their lean littermates (S1 Table). Twenty-week-old obese ZSF1 male rats demonstrated pancreatic dysfunction by showing a 2.7-fold elevation in systemic C-peptide (Fig 2A), a 47-fold increase in proinsulin (Fig 2B), a 6.3-fold increase in serum active amylin (Fig 2C), and elevated glucagon (37.8 ± 4.6 pg/mL in obese ZSF1 vs 25.8 ± 2.5 pg/mL in lean ZSF1 littermates; $p = 0.0388$; Fig 2D). Impaired renal function in the obese ZSF1 group was characterized with significantly increased serum kidney injury markers NGAL (1.5-fold vs lean ZSF1; Fig 2E), KIM-1 (2.2-fold

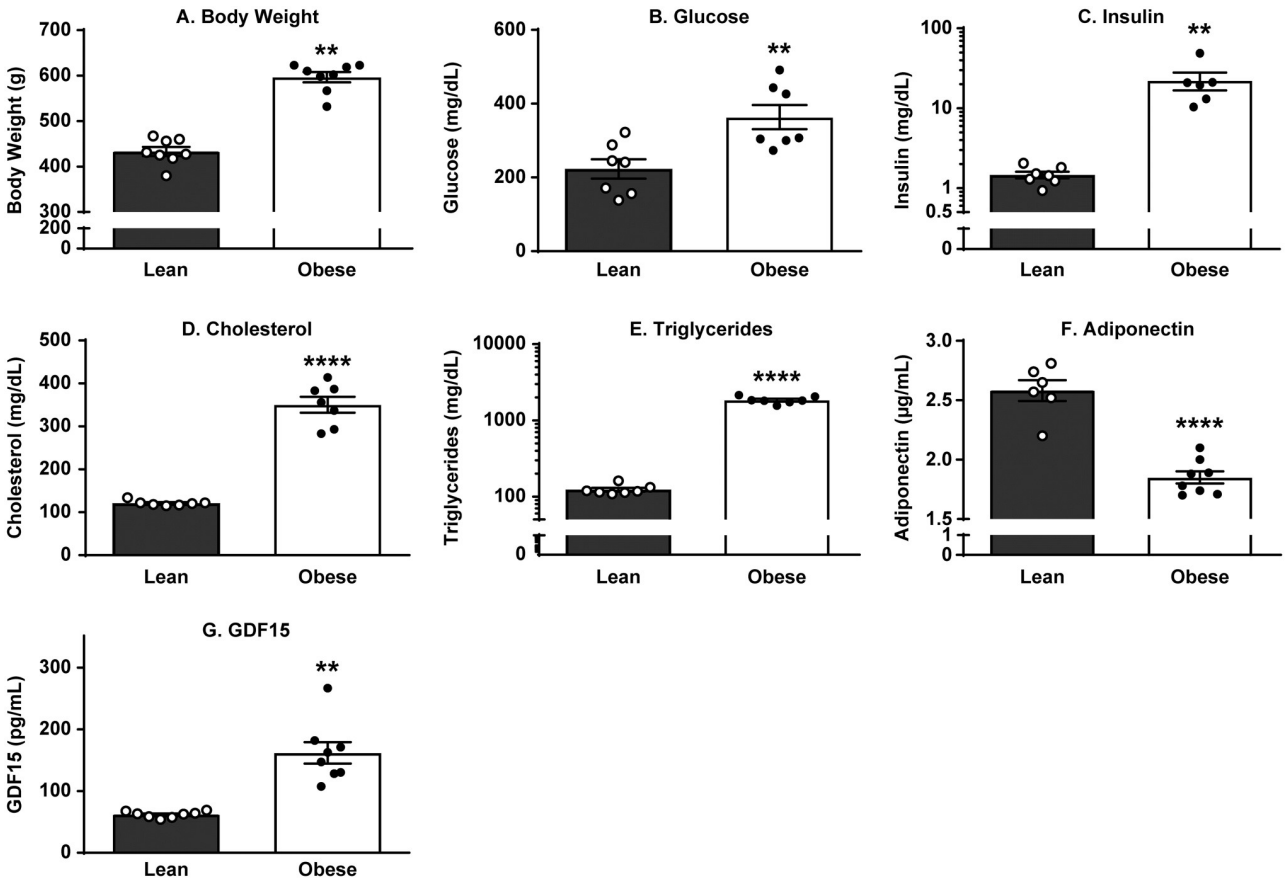

Fig 1. Obese ZSF1 male rats exhibited increased BW, glucose, insulin, cholesterol, and triglyceride levels and decreased adiponectin and increased GDF15 levels. Obese ZSF1 male rats at the age of 20 weeks exhibited increased body weight (A), elevated blood glucose (B), insulin (C), cholesterol (D), and triglyceride levels (E), decreased adiponectin (F), and increased growth differentiation factor 15 (GDF15) (G). Stars (*) indicate significance (** $p < 0.01$, **** $p < 0.0001$) by unpaired two-tailed *t* test. $n = 8$ for lean and $n = 8$ for obese ZSF1 groups.

https://doi.org/10.1371/journal.pone.0231234.g001

vs lean ZSF1; Fig 2F), and clusterin (1.4-fold vs lean ZSF1; Fig 2G). Renal biomarker changes documented above were confirmed with histopathological findings that were observed in kidneys of obese ZSF1 rats. These findings consisted of tubular ectasia, protein casts, tubular degeneration and regeneration, minimal interstitial fibrosis, infiltration by mononuclear inflammatory cells, and minimal glomerulosclerosis (Fig 2H).

Obese ZSF1 rats demonstrated impaired cardiac function and reduced exercise capacity at the age of 19–21 weeks

The complete set of invasive hemodynamic assessment, echocardiography, and exercise capacity of 20- to 21-week-old lean and obese ZSF1 male rats is presented in Table 1. The heart-to-brain weight ratios were significantly higher in obese ZSF1 male rats than in lean ZSF1 littermates. Invasive hemodynamic assessment at 21 weeks for rats anesthetized with ketamine/diazepam showed an increased relaxation constant *tau*. Echocardiography at 20 weeks under isoflurane anesthesia revealed that obese ZSF1 male rats exhibit a significant decrease in heart rate, ratio of mitral peak velocity of early filling to early diastolic mitral annular velocity (E/E'), and isovolumic relaxation time (IVRT), while maintaining a normal

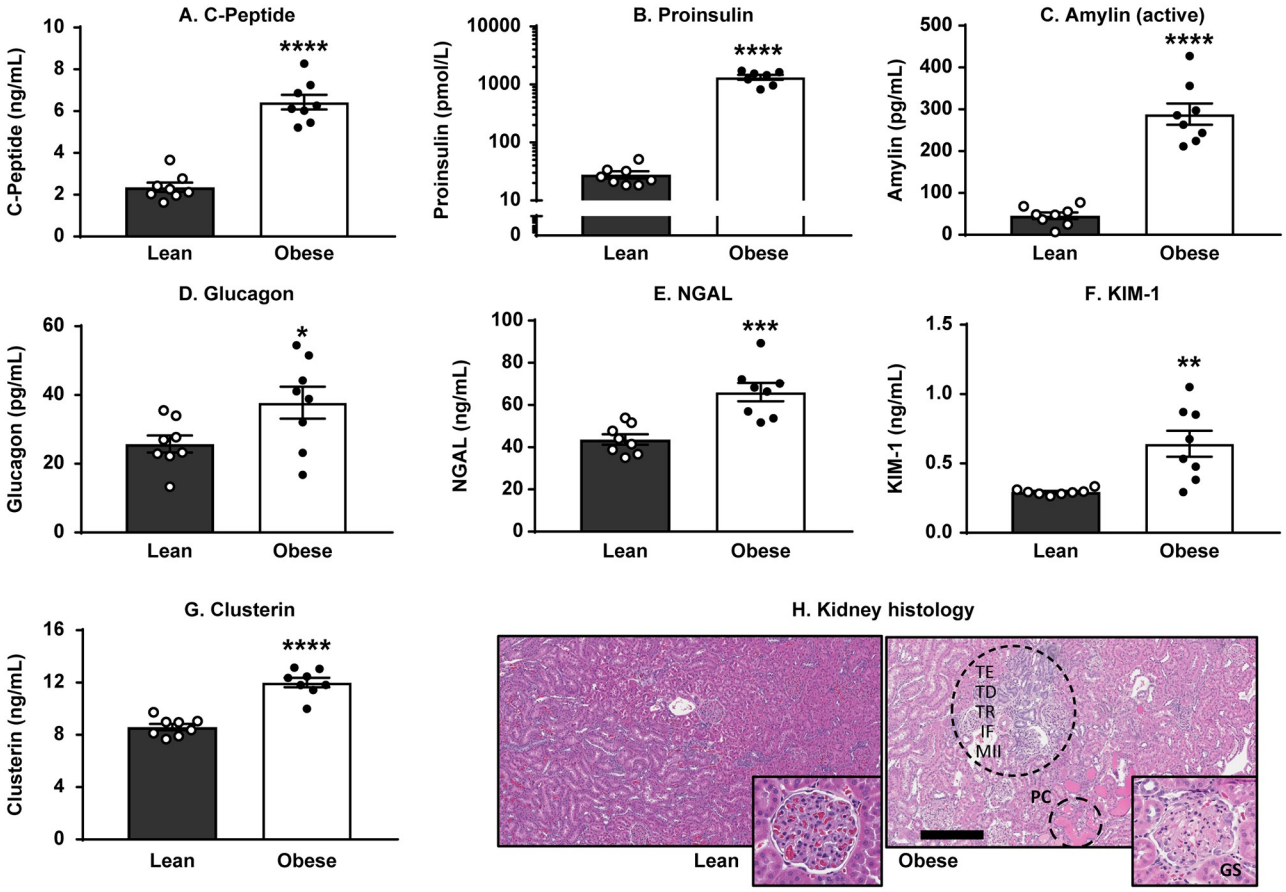

Fig 2. Obese ZSF1 rats demonstrated pancreatic dysfunction and impaired renal function. Obese ZSF1 rats show increased C-peptide (A), proinsulin (B), active amylin (C), and glucagon (D). Obese ZSF1 rats exhibit impaired renal function by showing increased serum levels of kidney injury markers NGAL (E), KIM-1 (F), and clusterin (G). Stars (*) indicate significance (* $p < 0.05$, ** $p < 0.01$, *** $p < 0.001$, **** $p < 0.0001$) by unpaired two-tailed *t* test. $n = 8$ for lean and $n = 8$ for obese ZSF1 groups. The following pathology was observed in obese ZSF1 kidneys (H): protein casts (PC), tubular ectasia (TE), tubular degeneration (TD) and regeneration (TR), minimal interstitial fibrosis (IF), infiltration by mononuclear inflammatory cells (MII), and minimal glomerulosclerosis. Bar = 300 μm.

https://doi.org/10.1371/journal.pone.0231234.g002

ejection fraction. We further demonstrated that obese ZSF1 male rats exhibit a limited exercise capacity with significantly shorter time to exhaustion, lower peak VO_2, and shorter distance following a treadmill exercise challenge.

An examination of obese ZSF1 females revealed that at 21 weeks of age, obese ZSF1 females weighed more than lean ZSF1 females (442 ± 4 g vs 246 ± 2 g) but weighed less than their male siblings (596 ± 11 g vs 433 ± 10 g; Fig 1A, S2 Table). Echocardiography at 21 weeks under isoflurane anesthesia revealed that ejection fraction and fractional shortening were comparable between lean and obese ZSF1 females (S2 Table). However, obese ZSF1 female rats exhibited a significant increase in LV mass that was associated with a significant decrease in heart rate and stroke volume and a significant prolongation in diastolic function and IVRT; E/E' ratio was comparable between the two groups (S2 Table). Consistent with our findings when comparing lean and obese ZSF1 males, we found that during an exercise challenge 19-week-old obese ZSF1 females exhibited reduced exercise capacity with significantly shorter running time, running distance, and a lower peak VO_2 compared with lean ZSF1 females (S2 Table).

Table 1. Obese ZSF1 male rats exhibited diastolic dysfunction and decreased exercise capacity.

Biomarker	Physical parameters (mean ± SEM)		*p*-value
	Lean ZSF1 (*n* = 8)	Obese ZSF1 (*n* = 8)	
Heart/brain weight (ratio)	**0.68 ± 0.03**	**0.81 ± 0.01**	***0.0070***
Heart rate (bpm)	**371.2 ± 9.5**	**292.8 ± 4.1**	***<0.0001***
Diameter (s) (mm)	3.59 ± 0.18	4.37 ± 0.34	0.053
Diameter (d) (mm)	**8.0 ± 0.13**	**9.21 ± 0.28**	***0.0011***
Volume (s) (μL)	**56.07 ± 6.29**	**91.23 ± 14.71**	***0.0383***
Volume (d) (μL)	**345.8 ± 11.94**	**474.8 ± 29.16**	***0.0009***
Stroke volume (μL)	**289.7 ± 10.0**	**383.5 ± 18.65**	***0.0005***
Ejection fraction (%)	83.93 ± 1.6	81.45 ± 2.32	0.3839
Fractional shortening (%)	50.03 ± 1.97	52.89 ± 2.56	0.4919
Cardiac output (mL/min)	107.4 ± 4.3	112 ± 5.1	0.4990
LV mass (mg)	1274 ± 124.2	1445 ± 41.1	0.2384
LV mass cor (mg)	1019 ± 99.4	1156 ± 32.9	0.2384
IVRT (ms)	**20.12 ± 0.55**	**24.89 ± 0.67**	***<0.0001***
EDP (mmHg)	1.808 ± 1.116	3.445 ± 1.342	0.3669
Tau (ms)	**6.83 ± 0.33**	**9.53 ± 46**	***0.0004***
E/E' (ratio)	**16.25 ± 1.07**	**25.07 ± 2.65**	***0.0064***
Distance (m)	**394.9 ± 27.9**	**194.0 ± 6.5**	***<0.0001***
Time to exhaustion (min)	**27.13 ± 1.34**	**17.75 ± 0.53**	***<0.0001***
Peak VO_2 (mg/kg/h)	**3541 ± 130**	**2927 ± 33.4**	***0.0004***
Respiratory exchange (ratio)	0.993 ± 0.017	0.9583 ± 0.015	0.1452

https://doi.org/10.1371/journal.pone.0231234.t001

At 20 weeks of age, obese ZSF1 male rats exhibited significant changes in major systemic biomarkers of cardiovascular function without histopathological changes in heart tissue

To evaluate the translational value of the obese ZSF1 rat model for human CMS, we next profiled major systemic CVD biomarkers (Fig 3A–3F, S3 Table) and compared the results with the gene expression of the same markers in the left heart of 20-week-old lean and obese ZSF1 male rats (Fig 3G–3K). The array of systemic changes in CVD-related biomarkers included increased blood levels of hypertension marker aldosterone (Fig 3A), elevated FABP3, a biomarker of heart pathology (Fig 3B), and significantly increased vascular markers IL-16 (Fig 3C) and ST2 (Fig 3D). Systemic concentration of NT-proBNP (Fig 3E) in obese ZSF1 rats was significantly lower than in the lean rats, and OPN (Fig 3F) level in circulation was not different between lean and obese ZSF1 rats. Gene expression of the above markers in the left heart was not different between lean and obese ZSF1 rats for FABP3, IL-16, IL1RL1 (ST2 protein), and NPPB (NT-proBNP protein) (Fig 3G–3J), whereas the local SPP1 mRNA expression (OPN gene) in both LA and LV was significantly elevated in obese ZSF1 rats (Fig 3K).

Next, we studied whether documented changes in systemic and local biochemical and molecular biomarkers reflected pathological events that occurred in the heart tissue. Histopathological evaluations of the hearts from lean (32-week-old) and obese ZSF1 rats at the ages of 20 and 32 weeks were performed on fixed tissues stained with standard hematoxylin and eosin or Picrosirius red (Fig 4). No evidence of fibrosis or chronic inflammation was detected in the hearts from lean or obese 20-week-old ZSF1 male rats (Fig 4A and 4B), whereas the hearts from 32-week-old obese rats exhibited mild interstitial fibrosis with infiltration by mononuclear inflammatory cells (mainly macrophages and lymphocytes) in the myocardium, including papillary muscles (Fig 4C). By quantitative evaluation, the collagen-occupied area in

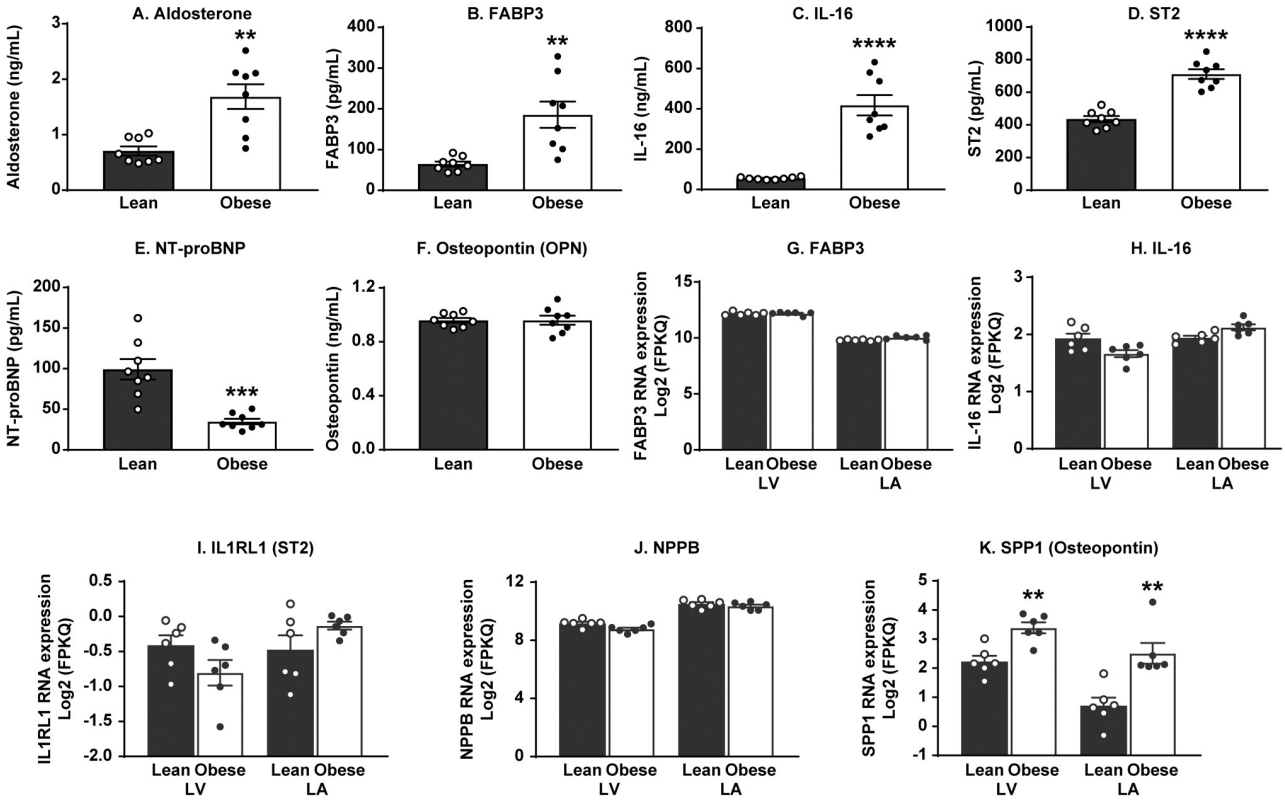

Fig 3. Twenty-week-old obese ZSF1 male rats exhibited cardiovascular dysfunction. Obese ZSF1 rats show increased blood levels of aldosterone (A), fatty-acid-binding protein 3 (FABP3; B), interleukin-16 (IL-16; C), and ST2 (IL1RL1 gene; D). In obese ZSF1 rats, systemic concentration of NT-proBNP (NPPB gene; E) is lower compared with the lean cohort and osteopontin (OPN; F) level in circulation is not different between the two cohorts. The mRNA expression of FABP3, IL-16, IL1RL1 (ST2 protein), and NPPB (NT-proBNP protein) in left heart was not different between lean and obese ZSF1 groups (G-J), whereas the local SPP1 (OPN protein) mRNA expression in left atria (LA) and left ventricle (LV) (K) was significantly elevated in obese ZSF1 rats. Stars (*) indicate significance (* $p < 0.05$, ** $p < 0.01$, *** $p < 0.001$, **** $p < 0.0001$) by unpaired two-tailed t test. $n = 8$ for lean and $n = 8$ for obese ZSF1 groups.

https://doi.org/10.1371/journal.pone.0231234.g003

the hearts of 32-week-old obese males was increased when compared to lean males (3.7% ± 0.38% vs 2.8% ± 0.35%) but did not achieve statistical significance ($p = 0.125$, Fig 4D).

CMS-related gene expression changes in the left heart of 20-week-old male ZSF1 rats

To characterize the transcriptional effects of obesity and metabolic dysfunction on the expression of left heart specific/abundant genes, RNA-seq was performed on LV isolated from 20-week-old lean and obese ZSF1 male rats (Fig 5). Comparison of heart abundant protein coding gene expression levels in LV biopsies from lean and obese ZSF1 rats revealed a relatively small number of genotype-driven gene expression changes (Fig 5A): the expression of 56 genes was significantly increased (FC > 1.5; $p < 0.05$; S6 Table), and the expression of 48 genes was significantly decreased (FC < 0.75; $p < 0.05$; S7 Table) in obese rats vs lean rats. The IPA pathway enrichment analysis of significantly dysregulated genes in the LV of obese ZSF1 rats revealed that the altered genes are significantly enriched in fatty acid and branched-chain amino acid (BCAA) metabolism pathways (Fig 5B). The increase in ACADM, EHHADH, HADHA, and HADHB gene expression was shared by both fatty acid and BCAA metabolism pathways. Altered ACAA2, ACOT2, ACSL6, ECI1, BDH1, HMGCS2, and IDI1 gene expression was fatty acid metabolism specific, and altered expression of DUSP26, MAOA, MAOB, PHGDH, and

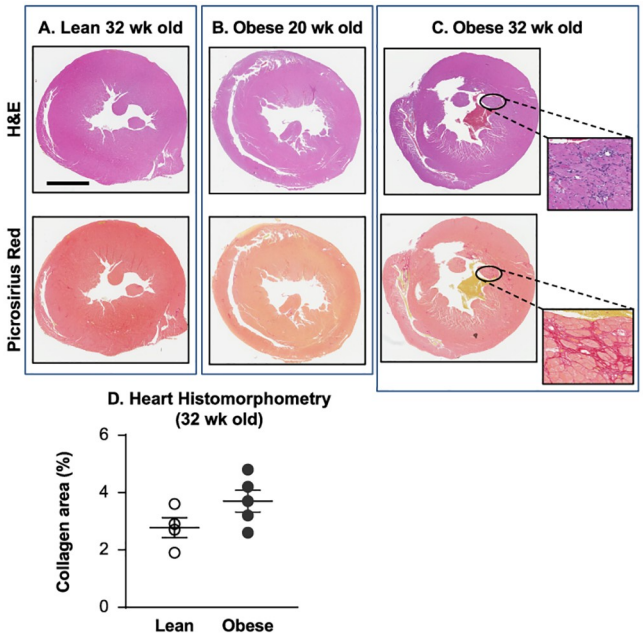

Fig 4. 20-week-old obese ZSF1 male rats did not exhibit histopathological events in heart tissue. Histopathological evaluation of the hearts from lean (32-week-old, $n = 4$) and obese ZSF1 rats at the ages of 20 ($n = 9$) and 32 ($n = 5$) weeks demonstrated no evidence of fibrosis or chronic inflammation in the hearts from lean (A) or obese (B) 20-week-old ZSF1 males, but the hearts from 32-week-old obese rats (C) exhibited mild interstitial fibrosis with infiltration by mononuclear inflammatory cells in the myocardium; percentage of the myocardial area occupied by collagen (D) in 32-week-old obese males was increased, but did not achieve statistical significance vs the lean group. Fixed heart tissues were stained with standard hematoxylin and eosin or Picrosirius red; bar = 5 mm.

https://doi.org/10.1371/journal.pone.0231234.g004

PSAT1 in LV was signatory for the BCAA metabolism pathway (Fig 5C). The unbiased search on MeSH disease terms indicated that altered genes are highly associated with HF, cardiomyopathy, hypertrophy, cardiac injury, hyperglycemia, hyperinsulinism, and lipid metabolism errors (Fig 5D). The gene expression profile reflects the crosstalk of obesity, diabetes, and CVD (Fig 5E). For instance, uncoupling protein 3 (UCP3), carnitine palmitoyltransferase 1A (CPT1A), and patatin like phospholipase domain containing 2 (PNPLA2), which are at the crossroad of defects in lipid metabolism, glucose metabolism, and heart injury, were increased in the LV of obese ZSF1 rats. Elevated levels of PDK4 and thioredoxin interacting protein (TXNIP), and decreased expression of the array of genes associated with both heart diseases and compromised glucose metabolism were observed (Fig 5E). Interestingly, altered genes and signaling pathways were also shared by different subtypes of CVD (Fig 5F). For example, decreased MYL2 and MYH6 gene expression coincided with increased RYR2, HCN4, CORIN, NPPA, ERBB2, and MYH7 gene expression in hypertrophic and/or dilated cardiomyopathy (Fig 5F).

Together, these data provide a compelling case that obese ZSF1 rats exhibit multiple features of human CMS, including pathological changes in circulating biomarkers and in the expression of heart abundant genes, cardiovascular dysfunction with preserved ejection fraction, and decreased exercise capacity.

Obese ZSF1 male rats treated with Fc-GDF15 for 12 weeks demonstrated significant metabolic improvement by changes in systemic parameters and biomarkers of obesity and metabolism impairments

For the duration of Fc-GDF15 or vehicle treatment, both groups of obese ZSF1 rats were monitored weekly for food intake and body weight and biweekly for blood levels of total

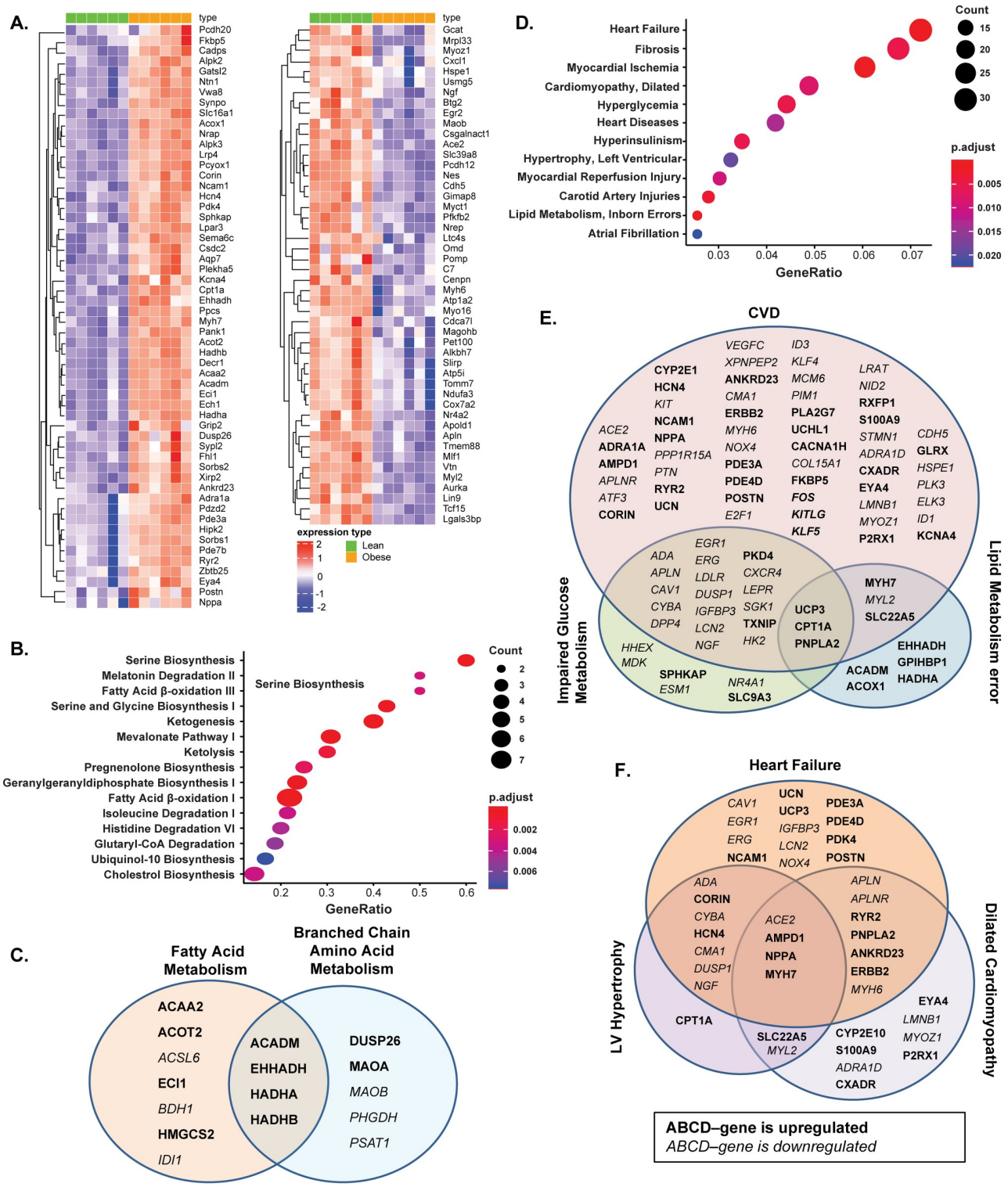

Fig 5. Gene expression analysis of RNA extracted from left ventricle (LV) of 20-week-old obese and lean ZSF1 male rats. The gene expression analysis of RNA revealed increased expression of 56 heart abundant genes and decreased expression of 48 heart abundant genes; the heatmap represents the individual expression changes in obese vs lean ZSF1 rats (A). Ingenuity pathway analysis (IPA) of enriched metabolic pathways (B) and comparison of differentially expressed genes (DEGs) presented in the enriched metabolic pathways from IPA over-represented cardiometabolic Medical Subject Headings (MeSH) terms (C). IPA of 267 significantly increased (FC > 1.5, Benjamini-Hochberg corrected p-value < 0.05) and 431 significantly decreased genes (FC < 2/3, p-value < 0.05) in LV of obese ZSF1 rats (D); comparison of DEGs enriched in cardiovascular disease (CVD), impaired

glucose metabolism, and lipid metabolism error disease pathways (E); and comparison of DEGs associated with different subgroups of heart disease pathways from over-representative MeSH term analysis (F). Gene symbols in bold indicate increase of expression and in italic indicate decrease of expression. $n = 8$ for lean and $n = 8$ for obese ZSF1 groups.

https://doi.org/10.1371/journal.pone.0231234.g005

cholesterol, triglycerides, insulin, and glucose (Fig 6). Within the first 2 weeks of Fc-GDF15 treatment, body weight (Fig 6A), food intake (Fig 6B), blood triglycerides (Fig 6C), and blood glucose levels (Fig 6D) decreased consistently until the end of the study. Blood cholesterol was 20–30% lower in the Fc-GDF15–treated obese ZSF1 rats (vs vehicle-treated animals) from week 1 to week 12 of the treatment (by two-way ANOVA: for fixed effects of treatment, $p = 0.0177$; for fixed effects of time, $p = 0.0130$; and for fixed effects of time x treatment, $p = 0.017$); however, this decrease did not achieve significance between the two groups at any tested time point of the study (Fig 6E). At the same time, insulin levels were significantly

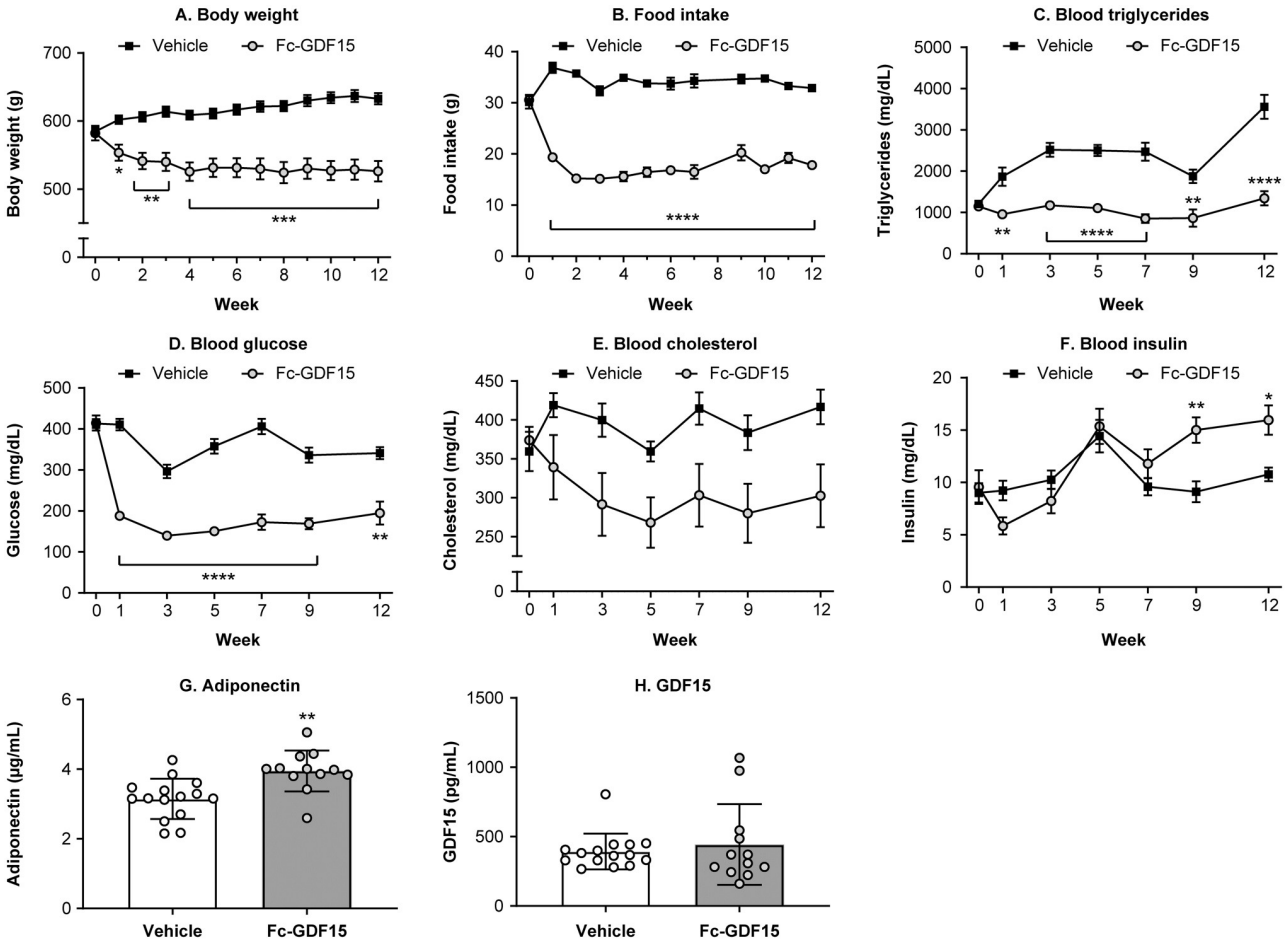

Fig 6. Effect of treatment of ZSF1 obese rats with Fc-GDF15 on systemic metabolic biomarkers. Treatment of ZSF1 rat with Fc-GDF15 resulted in decreased body weight (A) and food intake (B), decrease in blood triglyceride (C) and glucose levels (D), and trend in decrease of blood cholesterol (E). Blood insulin increased over time with GDF15 treatment (F). Twelve weeks of Fc-GDF15 treatment resulted in increased blood adiponectin (G) and had no effect on endogenous levels of rat GDF15 (H). When the effect in vehicle-treated and Fc-GDF15–treated obese ZSF1 rats was studied longitudinally (0–12 weeks), a two-way ANOVA with Sidak's multiple comparison test was performed for metabolic parameters, body weight, and food intake (A-F). Unpaired Student's *t* test was performed to evaluate the statistical significance between the groups at the end of a study (G, H). Stars (*) indicate significance ($^{*}\ p < 0.05$, $^{**}\ p < 0.01$, $^{***}\ p < 0.001$, $^{****}\ p < 0.0001$). $n = 15$ for the vehicle-treated obese ZSF1 group and $n = 12$ for the Fc-GDF15–treated obese ZSF1 group.

https://doi.org/10.1371/journal.pone.0231234.g006

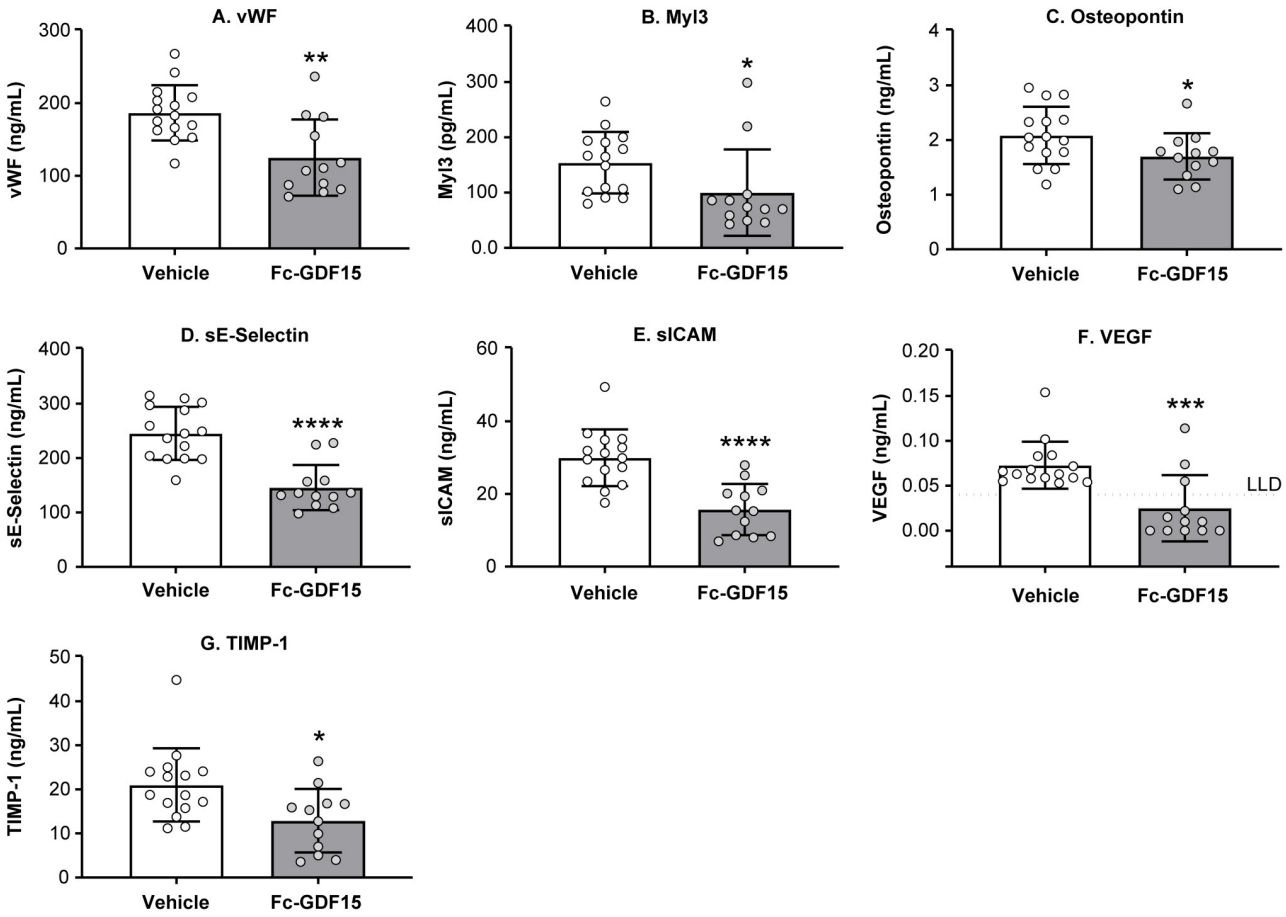

Fig 7. Effect of Fc-GDF15 treatment of ZSF1 obese rats on systemic CVD biomarkers. Obese ZSF1 rats treated with Fc-GDF15 for 12 weeks exhibit decrease in systemic levels of cardiovascular disease (CVD)–related biomarkers vWF (A), Myl3 (B), osteopontin (C), sE-selectin (D), sICAM (E), VEGF (F), and TIMP-1 (G) at the end of the study. Stars (*) indicate significance (* $p < 0.05$, ** $p < 0.01$, *** $p < 0.001$, **** $p < 0.0001$) by unpaired two-tailed t test. $n = 15$ for the vehicle-treated group and $n = 12$ for the Fc-GDF15–treated group.

https://doi.org/10.1371/journal.pone.0231234.g007

increased at weeks 9 and 12 of Fc-GDF15 treatment (Fig 6F). At the end of the 12-week Fc-GDF15 treatment, circulating adiponectin concentration was significantly increased (Fig 6G). Also, endogenous rat GDF15 levels in the serum of Fc-GDF15–treated and vehicle-treated obese ZSF1 rats remained similar (Fig 6H).

Fc-GDF15 treatment of obese ZSF1 rats led to significant changes in systemic levels of CVD-related biomarkers

Following 12 weeks of Fc-GDF15 administration, we observed significant changes in the array of cardiovascular circulating biomarkers. Thus, systemic markers of cardiac injury vWF (Fig 7A) and Myl3 (Fig 7B) were 30–50% lower ($p < 0.05$) in the Fc-GDF15 group. HF-associated OPN (Fig 7C), markers of vascular injury sE-selectin (Fig 7D), sICAM (Fig 7E), VEGF (Fig 7F), and marker of cardiovascular fibrosis TIMP-1 (Fig 7G) were significantly lower in the serum/plasma of Fc-GDF15–treated vs vehicle-treated obese ZSF1 rats ($p < 0.05$). At the same time, the other systemic biomarkers of CVD, such as NT-proBNP, NT-proANP, BNP, FABP3, MCP1, and aldosterone were not significantly changed by the 12-week–long Fc-GDF15 treatment (S4 Table).

Fc-GDF15 therapeutic approach affected echocardiography parameters of left heart function and improved exercise capacity in obese ZSF1 rats

When we characterized obese ZSF1 rats, we demonstrated that at the age of 20 weeks, males exhibited impaired cardiac function and decreased exercise capacity. Twelve weeks of Fc-GDF15 treatment of obese ZSF1 male rats resulted in significantly decreased heart-to-brain weight ratio (by echocardiography; Fig 8, S5 Table), LV mass (estimated by echocardiography), cardiac output, stroke volume, and ejection fraction when compared with obese ZSF1 rats treated with vehicle (Fig 8A–8E). Fc-GDF15 treatment had no effect on heart rate (Fig 8F). After 12 weeks of treatment, when exposed to a treadmill challenge, the Fc-GDF15 group demonstrated improved exercise capacity (S5 Table) by exhibiting significantly longer running time (Fig 8G) and running distance (Fig 8H) vs the vehicle group. However, peak VO_2 (a measure of aerobic fitness) and RER (a fatigue measure) were not significantly different between groups (S5 Table), suggesting that both groups were run to the same level of exhaustion.

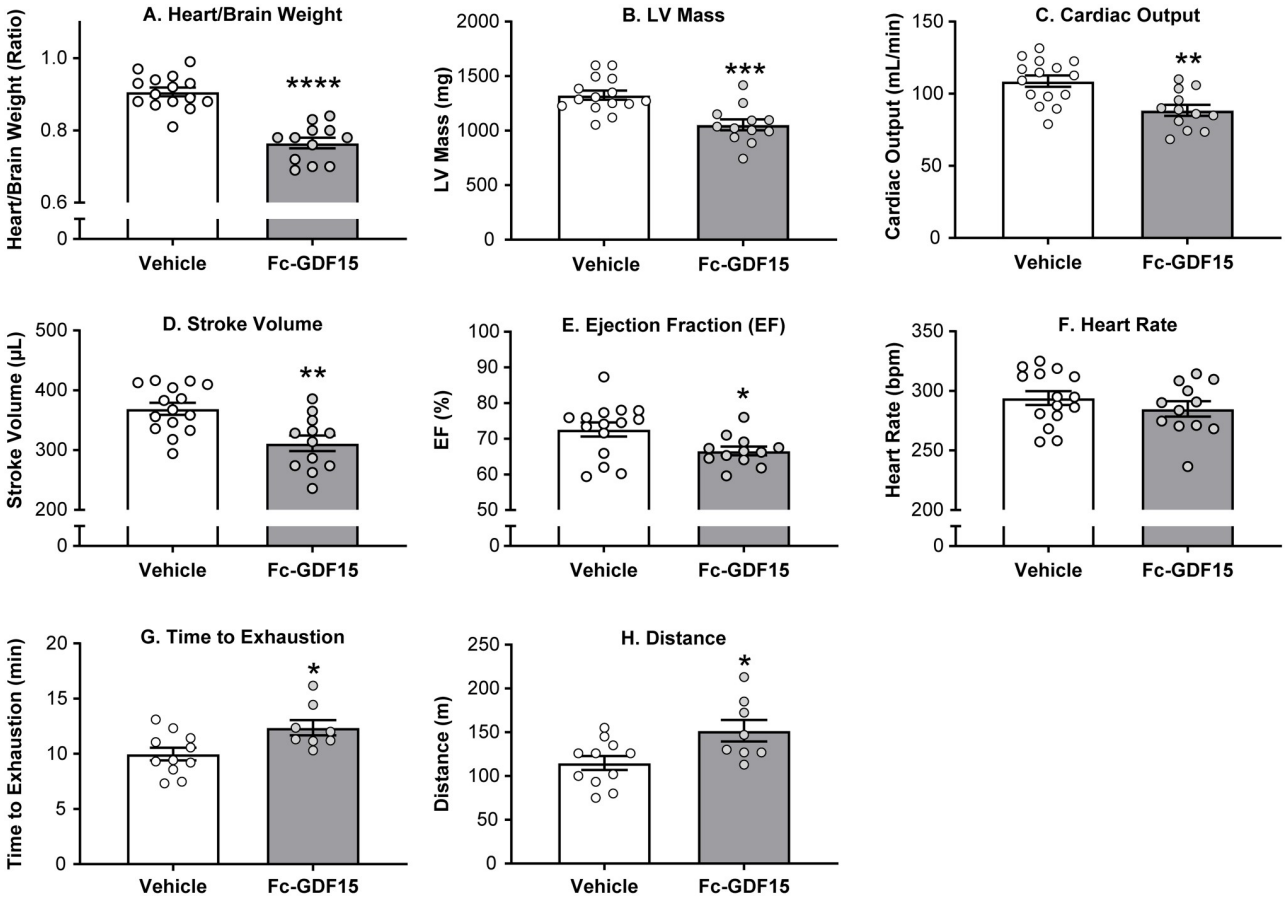

Fig 8. Fc-GDF15–treated obese ZSF1 rats demonstrated improved parameters of cardiac function and increased exercise capacity. Twelve weeks of Fc-GDF15 treatment decreased heart weight (A); decreased left ventricular (LV) mass (B), cardiac output (C), stroke volume (D), and ejection fraction (E) but not heart rate (F). Fc-GDF15–treated obese ZSF1 rats demonstrated improved exercise capacity during treadmill exercise by increased length of time to exhaustion (G) and running distance (H). Stars (*) indicate significance (* $p < 0.05$, ** $p < 0.01$, *** $p < 0.001$, **** $p < 0.0001$) by unpaired two-tailed *t* test. Parameters of cardiac function were evaluated in 15 vehicle-treated obese rats and in 12 Fc-GDF15–treated obese rats. Exercise capacity test was performed in 11 rats treated with vehicle and in 8 rats treated with Fc-GDF15.

https://doi.org/10.1371/journal.pone.0231234.g008

Discussion

CMS is a combination of primarily IR-associated metabolic disorders with a reciprocal relationship between impaired metabolism and HFpEF [3]. Our understanding of the pathophysiology and mechanisms of CMS-related HFpEF is limited due to the minimal availability of human myocardial biopsies and the lack of animal models that closely mimic human pathology.

Recently, obese ZSF1 rats were proposed as a robust CMS model because at the age of 20 weeks, males demonstrate hypertension, obesity, T2D, impaired metabolism, HF, and exercise intolerance [4, 7, 23, 31]. The use of male ZSF1 rats has been supported by several publications independent of our internal research [32, 33]. The LV hypertrophy, LA dilation, and increased myocardial stiffness due to myofilament changes (without significant interstitial fibrosis) are well documented in obese ZSF1 rats [8]. In our study, we have confirmed the previous observations (Figs 1 and 3).

A recent study comparing males to females found that 26-week-old obese ZSF1 female rats exhibit evidence of impaired cardiac function that is largely comparable to age-matched males [9]. Our examination of 19- to 21-week-old obese ZSF1 females was generally consistent with their observations. In both studies, obese female rats exhibited an increase in LV mass that likely contributed to a significant decrease in heart rate, increase in stroke volume and, in our study, a prolongation of IVRT. We did not observe an increase in the E/E' ratio in 21-week-old females as documented for 26-week-old animals; this difference may be due to the age of the animals assessed, as we found that obese ZSF1 males exhibited a more profound impairment in cardiac function as they aged.

When we examined systemic levels of pancreas-related biomarkers in obese ZSF1 male rats, we found evidence of pancreatic beta-cell dysfunction with significantly increased serum C-peptide, proinsulin, glucagon, and amylin (Fig 2A–2D). Since renal dysfunction is a part of CMS, Hamdani *et al.* [8] compared major parameters of kidney function in 20-week-old obese vs lean ZSF1 rats and reported hyperglycemia caused glycosuria, increased urine output, compensatory water intake, and proteinuria, suggesting the presence of diabetic nephropathy despite preserved creatinine clearance and plasma protein levels. Histopathological evaluation of kidneys from obese ZSF1 rats revealed the presence of tubular ectasia, protein casts, tubular degeneration and regeneration, minimal interstitial fibrosis, infiltration by mononuclear inflammatory cells, and minimal glomerulosclerosis (Fig 2H). Significantly increased systemic kidney injury biomarkers KIM-1, NGAL, and clusterin (Fig 2E–2G) confirmed the presence of diabetic nephropathy and kidney damage in 20-week-old obese ZSF1 male rats.

Since biomarkers have emerged as powerful diagnostic and/or prognostic tools for the variety of CVD in humans, we studied and analyzed in depth the milieu of systemic protein and local molecular cardiovascular biomarker changes (LV of the heart) triggered by the development of CMS in obese ZSF1 rats and evaluated the translational value of the observations. Notably, among the array of systemic changes we have documented is an increase in aldosterone (Fig 3A) together with significant attenuation of NT-proBNP (Fig 3E). The reciprocal relationship between systemic aldosterone and NT-proBNP was recently reported in a human CMS populational study ($n = 1674$; age $\geq$ 45 years) [34], where the authors demonstrated strong ($p < 0.001$) association of aldosterone increase with hypertension, obesity, chronic kidney disease, metabolic syndrome, high triglycerides, concentric LV hypertrophy, and atrial fibrillation. They also demonstrated reverse correlation between aldosterone and NT-proBNP. During the last decade, several scientific reports from human populational studies have demonstrated that serum NT-proBNP concentrations were relatively lower in overweight and obese patients [35–37], suggesting that natriuretic peptides may provide a link between the

heart and adipose tissue [38]. The observation that human subcutaneous adipose tissue from obese subjects with T2D exhibits markedly increased natriuretic peptide (NP) receptor expression and higher clearance of NT-proBNP from the circulation [39] may explain why we observed a significant decrease in serum NT-proBNP without NPPB mRNA expression changes in the left heart of obese ZSF1 rats (Fig 3E and 3J).

FABP3 is abundantly expressed in cardiomyocyte cytoplasm; its circulating level is positively correlated with LV mass index ($p < 0.0001$, $r = 0.7226$). Therefore, FABP3 was proposed as an early biomarker of myocardial injury in humans [40]. ST2, a circulating protein marker of cardiomyocyte stress and fibrosis, which increases in patients across a wide spectrum of CVDs, is now recommended by the American College of Cardiology Foundation and American Heart Association joint guidelines for additive risk stratification in patients with HF [41]. Chronic inflammation contributes to cardiac fibrosis, and systemic IL-16 levels are specifically elevated in HFpEF patients (compared with HF with reduced ejection fraction [HFrEF] and controls), with a significant association between serum IL-16 and indices of LV diastolic dysfunction (LAVI, E/E', and DWS) [42]. In concert with the published results from human studies, serum FABP3, IL-16 and ST2 protein concentrations were significantly elevated in 20-week-old obese ZSF1 male rats (Fig 3B–3D).

OPN (abundant kidney protein majorly synthesized in the loop of Henle) is among the biomarkers of HF progression; it is known to be expressed at medium levels in heart tissue by endothelial cells, cardiomyocytes, and fibroblasts. Several groups reported human plasma OPN elevation in patients with advanced HF [43] and specifically in HFpEF cohorts [44]. Lopez *et al.* [45] have reported no association of plasma OPN with HF, whereas the myocardial expression of OPN was highly elevated in HF patients ($p < 0.0001$). Our preclinical results confirm the latter report and provide, for the first time, evidence that myocardial OPN is upregulated in the heart of rats with features associated with HFpEF, as shown in murine models of HF [46].

Based on transcriptome analysis, approximately 60% ($n = 12{,}224$ of 19,613) of protein-coding genes are expressed in heart tissue [47]. Two hundred of these genes show an elevated expression in heart compared to other tissue types, and most of the corresponding proteins (localized in the cytoplasm and in the sarcomeres) are involved in muscle contraction, ion transport, and ATPase activity. Understanding the pathophysiology of cardiac alterations in CMS is critical. Our comparative RNA-seq analysis (lean vs obese ZSF1) of rat LV heart abundant genes revealed 267 significantly increased genes and 431 significantly decreased genes, of which 56 increased genes and 48 decreased genes are among the abundant genes in human heart (Fig 5A). Enriched signaling and disease pathway analyses added to our current understanding of how intermediary metabolism affects LV hypertrophy and influences heart tissue remodeling and repair. In the ZSF1 rat CMS model, obesity and impaired metabolism have also greatly increased CVD pathology by altering two major metabolic pathways in heart tissue (Fig 5B and 5C)—fatty acid metabolism and BCAA metabolism. In general, cardiac metabolic homeostasis of fatty acid, glucose, ketone bodies, and BCAAs is well established through intertwined regulatory networks [48, 49]. Thus, gene expression of essential enzymes involved in both fatty acid metabolism and BCAA catabolism—ACADM, EHHADH, HADHA, and HADHB—is greatly increased in obese ZSF1 LV heart tissue. It has been reported that acyl-CoA deficiency in human failing heart disrupts cardiac energy production and leads to cardiac lipotoxicity, which has a negative impact on the heart as it impairs its ability to function and pump properly [50]. ACAA2, ACADM, ACSL6, ACOT2, EHHADH, HADHA, and HADHB are enzymes functionally involved in acyl-CoA metabolism. Human genome-wide association studies (GWAS) have indicated that mutations in HADHA and HADHB are associated with familial hypertrophic cardiomyopathy [51], and

mutations in CPT1, ACADM, and ACAA2 genes are associated with impaired mitochondrial fatty acid β-oxidation [52]. Several enzymes (ACADM, ACSL6, EHHADH, and HMGCS2) are regulated by proliferator-activated receptors (PPARs), which manipulate the fuel supply and substrate and modulate HF progression [53, 54]. Based on the MeSH database analysis, we have demonstrated that in the obese ZSF1 rat model, the top representative diseases were CVD, hyperinsulinemia, hyperglycemia, and lipid metabolism defects (Fig 5D). Obesity and T2D are among the top drivers of HFpEF progression [2, 3]. Transcriptome profiling revealed the array of genes and pathways potentially mediating the cardiac metabolic shift, glucose and lipid toxicity, and the development of cardiomyopathy (Fig 5E). For instance, UCP3, CPT1A, and PNPLA2 are shared DEGs among impaired lipid metabolism, glucose metabolism, and CVD. CPT1A and UCP3 are involved in cardiac glucose oxidation, mitochondrial fatty acid oxidation, and ATP production. CPT1 inhibition has demonstrated beneficial effect in HF [55], and UCP3 was considered a marker for cellular metabolic state [56]. Mutations in PNPLA2 (which encodes adipose triglyceride lipase, ATGL) have been associated with triglyceride deposit cardiomyovasculopathy (TCGV) [57]. Mori *et al.* [58] have found that deletion of pyruvate dehydrogenase kinase 4 (PDK4) prevented angiotensin II-induced cardiac hypertrophy and improved cardiac glucose oxidation and energy usage. MeSH-based disease analysis demonstrated that significant changes in cardiomyocyte genes (decreased MYL2 and MYH6 and increased RYR2, HCN4, CORIN, NPPA, ERBB2, and MYH7) in LV of obese ZSF1 rats were strongly associated with dilated cardiomyopathy, LV hypertrophy, and HF (Fig 5F), and were similar to those observed in human genetic studies [59]. The array of expression changes in LV heart abundant genes in obese ZSF1 rats would help us to better understand the cardiac metabolic shift and cardiomyopathy in CMS; to allocate the major players mediating the crosstalk between glucose, lipid metabolism, and development of CVD; and to potentially identify key markers of cardiac energy status and heart injury grade. Notably, histopathological evidence of cardiac fibrosis or local chronic inflammation is not evident in the hearts of 20-week-old obese ZSF1 rats, when the gene expression changes are already present and documented (Fig 3). In addition, novel pathway (IPA), KEGG, and MeSH analyses demonstrate that heart tissue–specific gene expression changes in obese ZSF1 rats are driven by obesity and impaired metabolism, therefore, confirming the translational value of obese ZSF1 rat model for human CMS.

Hence, transcriptome profiling of lean and obese ZSF1 rats further supports the translational value of the obese ZSF1 CMS rat model in biomarker discovery and evaluation of therapeutic targets.

GDF15 is a distant member of the TGF-β superfamily. It is secreted, circulating in plasma as a 25 kDa homodimer [10, 11], and has become a novel exploratory biomarker of CMS because its circulating levels are increased in humans with metabolic syndrome [12, 15, 20] and in subjects with increased risk of CVD [13, 14]. In concert with human data, GDF15 levels do rise following a sustained high-fat diet or dietary amino acid imbalance in mice [60], and according to our present report (Fig 1G), GDF15 is significantly increased in the serum of obese ZSF1 rats. To date, GDF15 is positioned as a stress-induced hormone that mediates an aversive dietary response in preclinical species; when it was tested in obese mouse and non-human primate models, treatment resulted in significantly reduced body weight and food intake, increased energy expenditure, and improved glucose tolerance [15, 16].

Results reported here make a compelling case for obese ZSF1 rats exhibiting multiple features of human CMS, which include pathological changes in systemic renal, metabolic, and CVD circulating biomarkers, with features associated with HFpEF, and decreased exercise capacity. Recently published studies in obese preclinical models [15, 16, 60] demonstrated aversive dietary response to GDF15 treatment, leading to improvement in metabolic

parameters. We treated obese ZSF1 rats with Fc-GDF15 for 12 weeks and compared the outcome with that in vehicle-treated obese ZSF1 rats. Twelve-week Fc-GDF15 treatment resulted in a significant decrease in body weight and food intake, demonstrating its capacity to mediate aversive dietary response. Fc-GDF15 treatment did not lead to an increase in blood insulin from week 5 to week 9 and/or 12 (Fig 6F). Documented significance between the vehicle-treated group and the Fc-GDF15–treated group at weeks 9 and 12 of a treatment phase is rather due to the blood insulin decline in the vehicle-treated group. The latter observation together with significantly higher glucose levels in the vehicle-treated obese ZSF1 group (vs Fc-GDF15-treated) rather indicates progression of diabetes and deterioration and failing of pancreatic islets in aging obese ZSF1 rats. Fc-GDF15 improved metabolic parameters (decreased blood glucose and triglycerides) in obese ZSF1 rats (Fig 6A–6F), similar to previously reported results in diet-induced obese mice and obese cynomolgus monkeys [16], and significantly increased serum adiponectin in Fc-GDF15–treated obese ZSF1 rats. Adiponectin is mainly secreted by adipocytes, but also by skeletal muscle cells, cardiac myocytes, and endothelial cells. Reduction of adiponectin plays a central role in CMS because it is positively associated with insulin sensitivity [61] and shows anti-atherogenic and anti-inflammatory properties; according to numerous epidemiological studies, hypoadiponectinemia (adiponectin deficiency) is additionally associated with CVDs such as hypertension, coronary artery disease, and LV hypertrophy [62]. While circulating adiponectin was decreased by 30% in obese vs lean ZSF1 rats (Fig 1F), Fc-GDF15 treatment led to its significant systemic increase (29%; Fig 6G) vs obese ZSF1 rats treated with vehicle. Although Fc-GDF15 treatment did not lead to systemic changes in aldosterone, NT-proBNP, and FABP3 (S4 Table) in obese ZSF1 rats, the novel and exploratory systemic protein markers [63] of cardiac injury vWF and Myl3; HF-associated OPN; markers of vascular injury sE-selectin, sICAM, and VEGF; and cardiovascular fibrosis marker TIMP-1 were significantly lower in Fc-GDF15–treated obese rats vs vehicle-treated obese rats (Fig 7). Based on the moderate Fc-GDF15 treatment effect on systemic markers of heart function, we did not expect significant changes in local LV gene expression, and therefore, RNA-seq analysis was not performed.

In addition to the positive changes in the array of systemic cardiometabolic biomarkers, 12-week–long Fc-GDF15 therapy led to a considerable decrease in heart weight, improved parameters of LV function (decreased LV mass, cardiac output, and stroke volume; Fig 8), and increased exercise capacity (time to exhaustion and distance; Fig 8) when compared with vehicle-treated obese ZSF1 rats. It is worth noting that the Fc-GDF15–treated and the vehicle-treated rats were older at the time of the treadmill challenge relative to the obese ZSF1 rats from the first experiment (37 and 19 weeks, respectively). We believe that this resulted in reduced exercise capacity, differences in the heart/brain weight ratio, and differences in cardiovascular endpoints between the two studies. We believe that the modest but significant decrease in cardiac output, stroke volume, and ejection fraction that occurred is a consequence of the reduction in the size of the heart and is not enough to impair the ability of the heart to adequately oxygenate the animal.

Conclusion

In summary, the obese ZSF1 male rat represents a preclinical model with features associated with HFpEF that can mimic human CMS. Furthermore, Fc-GDF15 treatment of obese ZSF1 rats demonstrated its cardioprotective therapeutic effect in this model. These findings may have important clinical implications for potential pharmacologic treatment of obesity and associated comorbidities such as HF, where the unmet medical need remains high.

Supporting information

S1 File. Gene models used for alignment and quantification.
(DOCX)

S1 Table. Metabolic and renal biomarkers in serum/plasma of 20-week-old lean and obese ZSF1 male rats.
(DOCX)

S2 Table. Echocardiographic and exercise capacity parameters in lean and obese ZSF1 female rats.
(DOCX)

S3 Table. Cardiovascular biomarkers in circulation of 20-week-old lean and obese ZSF1 male rats.
(DOCX)

S4 Table. Effect of 12-week–long Fc-hGDF15 treatment on systemic levels of cardiovascular markers.
(DOCX)

S5 Table. Effect of 12-week–long Fc-hGDF15 treatment on parameters of invasive hemodynamic assessment, echocardiography, and exercise capacity of obese ZSF1 male rats.
(DOCX)

S6 Table. Heart abundant tissue gene expression increase in LV of obese vs lean ZSF1 groups.
(DOCX)

S7 Table. Heart abundant tissue gene expression decrease in LV of obese vs lean ZSF1 groups.
(DOCX)

Acknowledgments

The authors thank Cathryn M. Carter of Amgen Inc for editorial support; she received compensation as an employee of Amgen Inc.

Author Contributions

Conceptualization: Ying Zhang, YuMei Xiong, Yinhong Chen, Brandon Ason, Murielle M. Véniant.

Data curation: Marina Stolina, Xin Luo, Chun-Ya Han, Rhonda Chen, YuMei Xiong, Yinhong Chen, Jun Yin, Artem Shkumatov, Brandon Ason, Clarence Hale.

Formal analysis: Xin Luo, Denise Dwyer, Chun-Ya Han, Rhonda Chen, Ying Zhang, YuMei Xiong, Yinhong Chen, Jun Yin, Artem Shkumatov.

Methodology: Xin Luo, Denise Dwyer, Rhonda Chen, Ying Zhang, YuMei Xiong, Yinhong Chen, Brandon Ason.

Supervision: Clarence Hale, Murielle M. Véniant.

Visualization: Clarence Hale.

Writing – original draft: Marina Stolina.

Writing – review & editing: Chun-Ya Han, Rhonda Chen, Ying Zhang, YuMei Xiong, Yinhong Chen, Jun Yin, Brandon Ason, Clarence Hale, Murielle M. Véniant.

References

1. Kelli HM, Kassas I, Lattouf OM. Cardio metabolic syndrome: a global epidemic. J Diabetes Metab. 2015; 6(3).
2. Caleyachetty R, Thomas GN, Toulis KA, Mohammed N, Gokhale KM, Balachandran K, et al. Metabolically healthy obese and incident cardiovascular disease events among 3.5 million men and women. J Am Coll Cardiol. 2017; 70(12):1429–1437. https://doi.org/10.1016/j.jacc.2017.07.763 PMID: 28911506
3. von Bibra H, Paulus W, St John Sutton M. Cardiometabolic syndrome and increased risk of heart failure. Curr Heart Fail Rep. 2016; 13(5):219–229. https://doi.org/10.1007/s11897-016-0298-4 PMID: 27539049
4. Tofovic SP, Kusaka H, Kost CK Jr., Bastacky S. Renal function and structure in diabetic, hypertensive, obese ZDFxSHHF-hybrid rats. Ren Fail. 2000; 22(4):387–406. https://doi.org/10.1081/jdi-100100882 PMID: 10901178
5. Griffin KA, Abu-Naser M, Abu-Amarah I, Picken M, Williamson GA, Bidani AK. Dynamic blood pressure load and nephropathy in the ZSF1 (fa/fa cp) model of type 2 diabetes. Am J Physiol Renal Physiol. 2007; 293(5):F1605–1613. https://doi.org/10.1152/ajprenal.00511.2006 PMID: 17728379
6. Joshi D, Gupta R, Dubey A, Shiwalkar A, Pathak P, Gupta RC, et al. TRC4186, a novel AGE-breaker, improves diabetic cardiomyopathy and nephropathy in Ob-ZSF1 model of type 2 diabetes. J Cardiovasc Pharmacol. 2009; 54(1):72–81. https://doi.org/10.1097/FJC.0b013e3181ac3a34 PMID: 19546815
7. Conceicao G, Heinonen I, Lourenco AP, Duncker DJ, Falcao-Pires I. Animal models of heart failure with preserved ejection fraction. Neth Heart J. 2016; 24(4):275–286. https://doi.org/10.1007/s12471-016-0815-9 PMID: 26936157
8. Hamdani N, Franssen C, Lourenco A, Falcao-Pires I, Fontoura D, Leite S, et al. Myocardial titin hypophosphorylation importantly contributes to heart failure with preserved ejection fraction in a rat metabolic risk model. Circ Heart Fail. 2013; 6(6):1239–1249. https://doi.org/10.1161/CIRCHEARTFAILURE.113.000539 PMID: 24014826
9. Nguyen ITN, Brandt MM, van de Wouw J, van Drie RWA, Wesseling M, Cramer MJ, et al. Both male and female obese ZSF1 rats develop cardiac dysfunction in obesity-induced heart failure with preserved ejection fraction. PLoS One. 2020; 15(5):e0232399. https://doi.org/10.1371/journal.pone.0232399 PMID: 32374790
10. Tsai VW, Manandhar R, Jorgensen SB, Lee-Ng KK, Zhang HP, Marquis CP, et al. The anorectic actions of the TGFbeta cytokine MIC-1/GDF15 require an intact brainstem area postrema and nucleus of the solitary tract. PLoS One. 2014; 9(6):e100370. https://doi.org/10.1371/journal.pone.0100370 PMID: 24971956
11. Bottner M, Laaff M, Schechinger B, Rappold G, Unsicker K, Suter-Crazzolara C. Characterization of the rat, mouse, and human genes of growth/differentiation factor-15/macrophage inhibiting cytokine-1 (GDF-15/MIC-1). Gene. 1999; 237(1):105–111. https://doi.org/10.1016/s0378-1119(99)00309-1 PMID: 10524241
12. Ding Q, Mracek T, Gonzalez-Muniesa P, Kos K, Wilding J, Trayhurn P, et al. Identification of macrophage inhibitory cytokine-1 in adipose tissue and its secretion as an adipokine by human adipocytes. Endocrinology. 2009; 150(4):1688–1696. https://doi.org/10.1210/en.2008-0952 PMID: 19074584
13. Brown DA, Breit SN, Buring J, Fairlie WD, Bauskin AR, Liu T, et al. Concentration in plasma of macrophage inhibitory cytokine-1 and risk of cardiovascular events in women: a nested case-control study. Lancet. 2002; 359(9324):2159–2163. https://doi.org/10.1016/S0140-6736(02)09093-1 PMID: 12090982
14. Kempf T, Bjorklund E, Olofsson S, Lindahl B, Allhoff T, Peter T, et al. Growth-differentiation factor-15 improves risk stratification in ST-segment elevation myocardial infarction. Eur Heart J. 2007; 28(23):2858–2865. https://doi.org/10.1093/eurheartj/ehm465 PMID: 17977844
15. Tsai VWW, Husaini Y, Sainsbury A, Brown DA, Breit SN. The MIC-1/GDF15-GFRAL pathway in energy homeostasis: implications for obesity, cachexia, and other associated diseases. Cell Metab. 2018; 28(3):353–368. https://doi.org/10.1016/j.cmet.2018.07.018 PMID: 30184485
16. Xiong Y, Walker K, Min X, Hale C, Tran T, Komorowski R, et al. Long-acting MIC-1/GDF15 molecules to treat obesity: evidence from mice to monkeys. Sci Transl Med. 2017; 9(412).
17. Emmerson PJ, Wang F, Du Y, Liu Q, Pickard RT, Gonciarz MD, et al. The metabolic effects of GDF15 are mediated by the orphan receptor GFRAL. Nat Med. 2017; 23(10):1215–1219. https://doi.org/10.1038/nm.4393 PMID: 28846098

18. Hsu JY, Crawley S, Chen M, Ayupova DA, Lindhout DA, Higbee J, et al. Non-homeostatic body weight regulation through a brainstem-restricted receptor for GDF15. Nature. 2017; 550(7675):255–259. https://doi.org/10.1038/nature24042 PMID: 28953886

19. Mullican SE, Lin-Schmidt X, Chin C-N, Chavez JA, Furman JL, Armstrong AA, et al. GFRAL is the receptor for GDF15 and the ligand promotes weight loss in mice and nonhuman primates. Nat Med. 2017; 23:1150. https://doi.org/10.1038/nm.4392 PMID: 28846097

20. Mullican SE, Rangwala SM. Uniting GDF15 and GFRAL: therapeutic opportunities in obesity and beyond. Trends Endocrinol Metab. 2018; 29(8):560–570. https://doi.org/10.1016/j.tem.2018.05.002 PMID: 29866502

21. Chrysovergis K, Wang X, Kosak J, Lee SH, Kim JS, Foley JF, et al. NAG-1/GDF-15 prevents obesity by increasing thermogenesis, lipolysis and oxidative metabolism. Int J Obes (Lond). 2014; 38(12):1555–1564.

22. Chung HK, Ryu D, Kim KS, Chang JY, Kim YK, Yi HS, et al. Growth differentiation factor 15 is a myomitokine governing systemic energy homeostasis. J Cell Biol. 2017; 216(1):149–165. https://doi.org/10.1083/jcb.201607110 PMID: 27986797

23. LourenÇo André P, Falcão-Pires I, Cerqueira R, Fontoura D, Miranda D, Hamdani N, et al. Abstract 17471: The Obese Zsf1 Rat as a New Model of Heart Failure with Preserved Ejection Fraction Accompanying the Metabolic Syndrome. Circulation. 2012; 126(suppl_21):A17471–A17471.

24. OmicSoft. www.omicsoft.com/array-studio.php. Accessed 20 January 2020.

25. Li B, Dewey CN. RSEM: accurate transcript quantification from RNA-Seq data with or without a reference genome. BMC Bioinformatics. 2011; 12:323. https://doi.org/10.1186/1471-2105-12-323 PMID: 21816040

26. Love MI, Huber W, Anders S. Moderated estimation of fold change and dispersion for RNA-seq data with DESeq2. Genome Biol. 2014; 15(12):550. https://doi.org/10.1186/s13059-014-0550-8 PMID: 25516281

27. Consortium GTEx. The Genotype-Tissue Expression (GTEx) project. Nat Genet. 2013; 45(6):580–585. https://doi.org/10.1038/ng.2653 PMID: 23715323

28. Gu Z, Eils R, Schlesner M. Complex heatmaps reveal patterns and correlations in multidimensional genomic data. Bioinformatics. 2016; 32(18):2847–2849. https://doi.org/10.1093/bioinformatics/btw313 PMID: 27207943

29. Yu G. Using meshes for MeSH term enrichment and semantic analyses. Bioinformatics. 2018; 34 (21):3766–3767. https://doi.org/10.1093/bioinformatics/bty410 PMID: 29790928

30. Yu G, Wang LG, Han Y, He QY. clusterProfiler: an R package for comparing biological themes among gene clusters. OMICS. 2012; 16(5):284–287. https://doi.org/10.1089/omi.2011.0118 PMID: 22455463

31. Riehle C, Bauersachs J. Small animal models of heart failure. Cardiovasc Res. 2019; 115(13):1838–1849. https://doi.org/10.1093/cvr/cvz161 PMID: 31243437

32. van Dijk CG, Oosterhuis NR, Xu YJ, Brandt M, Paulus WJ, van Heerebeek L, et al. Distinct endothelial cell responses in the heart and kidney microvasculature characterize the progression of heart failure with preserved ejection fraction in the obese ZSF1 rat with cardiorenal metabolic syndrome. Circ Heart Fail. 2016; 9(4):e002760. https://doi.org/10.1161/CIRCHEARTFAILURE.115.002760 PMID: 27056881

33. Brandt MM, Nguyen ITN, Krebber MM, van de Wouw J, Mokry M, Cramer MJ, et al. Limited synergy of obesity and hypertension, prevalent risk factors in onset and progression of heart failure with preserved ejection fraction. J Cell Mol Med. 2019; 23(10):6666–6678. https://doi.org/10.1111/jcmm.14542 PMID: 31368189

34. Buglioni A, Cannone V, Cataliotti A, Sangaralingham SJ, Heublein DM, Scott CG, et al. Circulating aldosterone and natriuretic peptides in the general community: relationship to cardiorenal and metabolic disease. Hypertension. 2015; 65(1):45–53. https://doi.org/10.1161/HYPERTENSIONAHA.114.03936 PMID: 25368032

35. Bayes-Genis A, Lloyd-Jones DM, van Kimmenade RR, Lainchbury JG, Richards AM, Ordonez-Llanos J, et al. Effect of body mass index on diagnostic and prognostic usefulness of amino-terminal pro-brain natriuretic peptide in patients with acute dyspnea. Arch Intern Med. 2007; 167(4):400–407. https://doi.org/10.1001/archinte.167.4.400 PMID: 17325303

36. Neeland IJ, Winders BR, Ayers CR, Das SR, Chang AY, Berry JD, et al. Higher natriuretic peptide levels associate with a favorable adipose tissue distribution profile. J Am Coll Cardiol. 2013; 62(8):752–760. https://doi.org/10.1016/j.jacc.2013.03.038 PMID: 23602771

37. Fedele D, Bicchiega V, Collo A, Barutta F, Pistone E, Gruden G, et al. Short term variation in NTproBNP after lifestyle intervention in severe obesity. PloS One. 2017; 12(7):e0181212. https://doi.org/10.1371/journal.pone.0181212 PMID: 28704534

38. Pivovarova O, Gogebakan O, Kloting N, Sparwasser A, Weickert MO, Haddad I, et al. Insulin up-regulates natriuretic peptide clearance receptor expression in the subcutaneous fat depot in obese subjects: a missing link between CVD risk and obesity? J Clin Endocrinol Metab. 2012; 97(5):E731–739. https://doi.org/10.1210/jc.2011-2839 PMID: 22419733

39. Kovacova Z, Tharp WG, Liu D, Wei W, Xie H, Collins S, et al. Adipose tissue natriuretic peptide receptor expression is related to insulin sensitivity in obesity and diabetes. Obesity (Silver Spring). 2016; 24 (4):820–828.

40. Varrone F, Gargano B, Carullo P, Di Silvestre D, De Palma A, Grasso L, et al. The circulating level of FABP3 is an indirect biomarker of microRNA-1. J Am Coll Cardiol. 2013; 61(1):88–95. https://doi.org/10.1016/j.jacc.2012.08.1003 PMID: 23141496

41. Daniels LB Antoni B-G. Using ST2 in cardiovascular patients: a review. Future Cardiol. 2014; 10 (4):525–539 https://doi.org/10.2217/fca.14.36 PMID: 25301315

42. Tamaki S, Mano T, Sakata Y, Ohtani T, Takeda Y, Kamimura D, et al. Interleukin-16 promotes cardiac fibrosis and myocardial stiffening in heart failure with preserved ejection fraction. PLoS One. 2013; 8(7): e68893. https://doi.org/10.1371/journal.pone.0068893 PMID: 23894370

43. Rosenberg M, Zugck C, Nelles M, Juenger C, Frank D, Remppis A, et al. Osteopontin, a new prognostic biomarker in patients with chronic heart failure. Circ Heart Fail. 2008; 1(1):43–49. https://doi.org/10.1161/CIRCHEARTFAILURE.107.746172 PMID: 19808269

44. Coculescu BI, Manole G, Dinca GV, Coculescu EC, Berteanu C, Stocheci CM. Osteopontin—a biomarker of disease, but also of stage stratification of the functional myocardial contractile deficit by chronic ischaemic heart disease. J Enzyme Inhib Med Chem. 2019; 34(1):783–788. https://doi.org/10.1080/14756366.2019.1587418 PMID: 30843743

45. Lopez B, Gonzalez A, Lindner D, Westermann D, Ravassa S, Beaumont J, et al. Osteopontin-mediated myocardial fibrosis in heart failure: a role for lysyl oxidase? Cardiovasc Res. 2013; 99(1):111–120. https://doi.org/10.1093/cvr/cvt100 PMID: 23619422

46. Xie Z, Singh M, Singh K. Osteopontin modulates myocardial hypertrophy in response to chronic pressure overload in mice. Hypertension. 2004; 44(6):826–831. https://doi.org/10.1161/01.HYP.0000148458.03202.48 PMID: 15534078

47. The Human Protein Atlas. https://www.proteinatlas.org/humanproteome/tissue/heart. Accessed 20 January 2020.

48. Gibb AA, Hill BG. Metabolic coordination of physiological and pathological cardiac remodeling. Circ Res. 2018; 123(1):107–128. https://doi.org/10.1161/CIRCRESAHA.118.312017 PMID: 29929976

49. Tobias DK, Lawler PR, Harada PH, Demler OV, Ridker PM, Manson JE, et al. Circulating branched-chain amino acids and incident cardiovascular disease in a prospective cohort of US women. Circ Genom Precis Med. 2018; 11(4):e002157. https://doi.org/10.1161/CIRCGEN.118.002157 PMID: 29572205

50. Goldenberg JR, Carley AN, Ji R, Zhang X, Fasano M, Schulze PC, et al. Preservation of acyl coenzyme A attenuates pathological and metabolic cardiac remodeling through selective lipid trafficking. Circulation. 2019; 139(24):2765–2777. https://doi.org/10.1161/CIRCULATIONAHA.119.039610 PMID: 30909726

51. Choi J-H, Yoon H-R, Kim G-H, Park S-J, Shin Y-L, Yoo H-W. Identification of novel mutations of the HADHA and HADHB genes in patients with mitochondrial trifunctional protein deficiency. Int J Mol Med. 2007; 19:81–87. PMID: 17143551

52. Das AM, Steuerwald U, Illsinger S. Inborn errors of energy metabolism associated with myopathies. J Biomed Biotechnol. 2010; 2010:340849. https://doi.org/10.1155/2010/340849 PMID: 20589068

53. Ichikawa T, Kita M, Matsui TS, Nagasato AI, Araki T, Chiang SH, et al. Vinexin family (SORBS) proteins play different roles in stiffness-sensing and contractile force generation. J Cell Sci. 2017; 130(20):3517–3531. https://doi.org/10.1242/jcs.200691 PMID: 28864765

54. Liao HH, Jia XH, Liu HJ, Yang Z, Tang QZ. The role of PPARs in pathological cardiac hypertrophy and heart failure. Curr Pharm Des. 2017; 23(11):1677–1686. https://doi.org/10.2174/1381612822666160928150040 PMID: 27779079

55. Fillmore N, Lopaschuk GD. Targeting mitochondrial oxidative metabolism as an approach to treat heart failure. Biochim Biophys Acta. 2013; 1833(4):857–865. https://doi.org/10.1016/j.bbamcr.2012.08.014 PMID: 22960640

56. Hilse KE, Rupprecht A, Egerbacher M, Bardakji S, Zimmermann L, Wulczyn A, et al. The expression of uncoupling protein 3 coincides with the fatty acid oxidation type of metabolism in adult murine heart. Front Physiol. 2018; 9:747. https://doi.org/10.3389/fphys.2018.00747 PMID: 29988383

57. Li M, Hirano KI, Ikeda Y, Higashi M, Hashimoto C, Zhang B, et al. Triglyceride deposit cardiomyovasculopathy: a rare cardiovascular disorder. Orphanet J Rare Dis. 2019; 14(1):134. https://doi.org/10.1186/s13023-019-1087-4 PMID: 31186072

58. Mori J, Alrob OA, Wagg CS, Harris RA, Lopaschuk GD, Oudit GY. ANG II causes insulin resistance and induces cardiac metabolic switch and inefficiency: a critical role of PDK4. Am J Physiol Heart Circ Physiol. 2013; 304(8):H1103–1113. https://doi.org/10.1152/ajpheart.00636.2012 PMID: 23396452

59. Tobita T, Nomura S, Fujita T, Morita H, Asano Y, Onoue K, et al. Genetic basis of cardiomyopathy and the genotypes involved in prognosis and left ventricular reverse remodeling. Sci Rep. 2018; 8(1):1998. https://doi.org/10.1038/s41598-018-20114-9 PMID: 29386531

60. Patel S, Alvarez-Guaita A, Melvin A, Rimmington D, Dattilo A, Miedzybrodzka EL, et al. GDF15 provides an endocrine signal of nutritional stress in mice and humans. Cell Metab. 2019; 29(3):707–718. e708. https://doi.org/10.1016/j.cmet.2018.12.016 PMID: 30639358

61. Yamauchi T, Kamon J, Waki H, Terauchi Y, Kubota N, Hara K, et al. The fat-derived hormone adiponectin reverses insulin resistance associated with both lipoatrophy and obesity. Nat Med. 2001; 7:941–946. https://doi.org/10.1038/90984 PMID: 11479627

62. Achari AE, Jain SK. Adiponectin, a therapeutic target for obesity, diabetes, and endothelial dysfunction. Int J Mol Sci. 2017; 18(6).

63. Upadhyay RK. Emerging risk biomarkers in cardiovascular diseases and disorders. J Lipids. 2015; 2015:971453. https://doi.org/10.1155/2015/971453 PMID: 25949827